Neuronal Changes Underlying Altered Biophysical Properties of Reticulospinal Neurons Following Spinal Cord Injury in the Lamprey

A Thesis

Presented to

the Faculty of the Graduate School

at the University of Missouri - Columbia

In Partial Fulfillment

of the Requirements for the Degree

Master of Arts

By

RYAN ANTHONY HOUGH

Dr. Andrew McClellan, Thesis Supervisor

JULY 2017

The undersigned, appointed by the dean of the Graduate School, have examined the thesis entitled

Neuronal Changes Underlying Altered Biophysical Properties of Reticulospinal Neurons Following Spinal Cord Injury in the Lamprey

Presented by Ryan Anthony Hough

A candidate for the degree of Master of Arts,

And hereby certify that, in their opinion, it is worth of acceptance

_____

Dr. Andrew McClellan

_____

Dr. David Schulz

_____

Dr. David Kline

ACKNOWLEDGEMENTS

I would like to acknowledge Dr. Andrew McClellan for his devotion to helping me grow as a student and as a developing professional. Additionally, I would like to thank Dr. David Schulz and Dr. David Kline for serving on my committee and helping me generate new and exciting ideas. Finally, I would like to thank my friends and family for their unwavering support in all that I do.

TABLE OF CONTENTS

ACKNOWLEDGEMENTS…… ii

LIST OF TABLES AND FIGURES…….. iv

ABSTRACT……. v

CHAPTER

1. **Introduction……. 1**
2. **Methods…… 18**
3. **Results…….. 30**
4. **Discussion…… 69**

REFERENCE LIST…… 81

LIST OF FIGURES AND TABLES

Figures		Page
1	Simplified model of a locomotor system in the lamprey	14
2	Dorsal surface of the brain of a larval lamprey	16
3	Isolated lamprey brain-spinal cord preparations	28
4	Repetitive firing and afterpotentials for uninjured and injured RS neurons	42
5	Membrane potential (V_m) and V-I plots for uninjured and injured RS neurons in response to hyperpolarizing and depolarizing current pulses	44
6	Histograms showing depolarizing membrane potential and current required for uninjured and injured RS neurons to reach threshold (V_{th})	46
7	Responses of uninjured and injured RS neurons to triangle current waveforms	48
8	Pharmacology of the delayed membrane repolarization	50
9	Correlation of amplitudes of delayed repolarization and corresponding firing patterns for injured RS neurons	52
10	Voltage clamp recordings and I-V plot for uninjured and injured RS neurons in response to voltage pulses up to threshold (V_{th})	54
11	Voltage clamp recordings and I-V plot for an uninjured and injured RS neuron below and above (V_{th})	56
12	Histograms showing resting membrane potentials (V_{rest}) and differences in effective activation voltages of outward rectifying current for uninjured and injured RS neurons	58
13	I-V plot for an injured RS neuron to determine the pharmacology of the outward rectifying current	60
14	Time course of the effect of TTX for an uninjured RS neuron	62
15	Injury phenotype induced by blocking SK channels and partially blocking voltage-gated sodium channels	64

Tables		Page
1	Biophysical properties of uninjured and injured RS neurons	66
2	Properties of delayed repolarization for injured RS neurons and their corresponding repetitive firing patterns	67
3	Biophysical properties of uninjured RS neurons in response to blocking SK channels and partially blocking Na^+ channels	68

ABSTRACT

Following severe spinal cord injury (SCI), the descending axons of reticulospinal (RS) neurons are disrupted and can no longer activate spinal locomotor neural circuits, thus interrupting brain-spinal cord commands for locomotion. For higher vertebrates, including humans, the descending axons of RS neurons are unable to regenerate, resulting in permanent paralysis below the site of the spinal lesion (Schwab and Bartholdi, 1996). In contrast, the central nervous system (CNS) of some lower vertebrates, including the lamprey, is permissive for axonal regeneration, and dramatically following SCI, voluntary locomotor control recovers below the healed spinal lesion site within about 8 weeks (reviewed in McClellan, 2013).

To understand the mechanisms by which lamprey RS neurons are able to display such an incredible regenerative response to injury, it is first important to investigate the neuronal changes that occur for injured neurons following SCI. In response to SCI, injured lamprey RS neurons undergo several dramatic changes in their biophysical properties that collectively are referred to as the "injury phenotype". For example, relative to uninjured RS neurons, injured neurons display a larger fast afterhyperpolarization (fAHP), a smaller or often absent afterdepolarization (ADP) and slow afterhyperpolarization (sAHP), as well as altered repetitive firing properties (McClellan et al., 2008). In addition, following SCI lamprey RS neurons display decreased excitability and altered firing patterns in response to depolarizing stimuli (McClellan et al., 2008). These biophysical changes are likely important for creating a cellular environment that is supportive for axonal regeneration. With the exception of the reduced or absent sAHP, it is not yet clear what neuronal changes occur to mediate all of

the components of the “injury phenotype”.

In the present study, neurophysiological experiments indicated that relative to uninjured lamprey RS neurons, injured neurons display several dramatic changes in their biophysical properties: (a) decreased membrane resistance, and increased capacitance and time constant; (b) increased voltage and current thresholds; (c) larger amplitudes for action potentials; and (d) higher slope of the repolarizing phase of action potentials. These changes in properties are expected to reduce excitability of injured RS neurons relative to uninjured neurons.

Current clamp and voltage clamp experiments were preformed to investigate if a possible up-regulation of outward rectifying potassium channels might contribute to the “injury phenotype”. The results indicated that for injured RS neurons, a delayed membrane repolarization was activated at depolarizing potentials just below as well as above threshold for APs, while for uninjured neurons the repolarization was mostly absent below threshold. In addition, the delayed repolarization was determined to be due to a delayed outward current. Because of the delayed membrane repolarization and delayed outward current, injured RS neurons resisted depolarization to threshold and were therefore less excitable than uninjured RS neurons. Pharmacological experiments indicated that after a block of voltage-gated sodium and calcium channels, the delayed membrane repolarization and delayed outward current were still observed for injured RS neurons and also were present for uninjured neurons, but mostly for membrane potentials above threshold. After a block of voltage-gated potassium channels, the delayed membrane repolarization and delayed outward current were significantly reduced, suggesting that these were produced by delayed outward rectifying potassium channels.

Thus, it appears that following SCI, there might be an up-regulation of these channels for injured lamprey RS neurons to reduce excitability.

Additional experiments were performed to investigate the modulation of voltage-gated sodium channels in response to SCI. As previously mentioned, some of the biophysical changes that comprise the "injury phenotype" suggest an up-regulation of a hyperpolarizing potassium channel. However, other components of the injury phenotype, such as a larger action potential amplitude, also suggest an up-regulation of voltage-gated sodium channels. In the present study, we hypothesized that both of these channels possibly are up-regulated, but there might be a differential increase in voltage-gated potassium channel conductance relative to that for voltage-gated sodium channels. This hypothesis was tested by applying low doses of TTX to *uninjured* RS neurons to partially block voltage-gated sodium channels. This experimental paradigm indicated that a pharmacologically-mediated decrease in conductance of sodium channels relative to potassium channels induced the injury phenotype for *uninjured* RS neurons, including changes in repetitive firing patterns and membrane resonance consistent with those for injured neurons.

Together, the changes in biophysical properties of injured lamprey RS neurons that occur following SCI appear to be important for limiting calcium influx. For example, the sAHP, which is reduced following injury, is mediated by high-voltage activated (HVA) calcium and calcium-activated potassium (SK) channels (McClellan et al., 2008). Additionally, the mRNA expression for these channels is significantly reduced following injury (McClellan et al., 2008). Data from the present study indicates that in addition to limiting calcium influx by down-regulating calcium channels, injured RS neurons also

reduce calcium influx by decreasing membrane excitability, possibly due to up-regulating outward rectifying potassium channels.

The many biophysical changes that comprise the "injury phenotype" provide insights into the conditions that are supportive for axonal regeneration for injured lamprey RS neurons following SCI. The electrophysiological and pharmacological data from the present study provide valuable information concerning how the changes in biophysical properties displayed by lamprey RS neurons contribute to the "injury phenotype" and how these altered properties might contribute to successful axonal regeneration. Ultimately, this and other knowledge will be critical for developing therapies to promote axonal regeneration and treat SCI in higher vertebrates, including hopefully one day, humans.

INTRODUCTION

Across the animal kingdom, locomotor behavior takes many forms, including swimming for fish, flying for birds, and walking for bipedal and quadrupedal terrestrial animals. In all cases, animals depend on locomotion to move about their environments in search of important elements of survival, such as food, water, shelter, and mates. Because this behavior is so critical, diseases or injuries that impair locomotion are often fatal for animals in the wild, or severely disabling for humans. To better treat these injuries in humans, it is important to understand the neural control of locomotion, and the changes that occur within this system following injury or disease.

Basic Organization of Locomotor Command Systems

Despite the different appearances of various forms of locomotion, the neural networks underlying these behaviors share many similarities. For example, locomotion is initiated by a "brain locomotor command system", which includes higher-order locomotor centers that activate reticulospinal (RS) neurons. The RS neurons send descending projections to the spinal cord to activate central pattern generators (CPGs) and initiate locomotion. Spinal CPGs are neural networks that can produce the basic rhythmic locomotor output, even in the absence of sensory feedback (reviewed in Orlovsky et al., 1999), although sensory feedback is necessary to modulate CPGs and adapt the locomotor output to the ongoing needs of the animal. Spinal CPGs produce the rhythmic motor pattern for locomotion, and it is thought that a similar neural network also produces the motor output for other rhythmic motor acts, such as scratching and wiping (reviewed in Grillner and Wallén, 1985).

Organization of Locomotor Command Systems for Higher Vertebrates

For many higher vertebrates, locomotion can be initiated by focal stimulation of higher-order brain locomotor centers. For example, stimulation of the mesencephalic locomotor region (MLR) (Garcia-Rill et al., 1983; Steeves and Jordan, 1984), the subthalamic locomotor region (SLR) (Waller, 1940; Orlovsky, 1969), as well as the fastigial nucleus of the cerebellum (Walberg et al., 1962) initiates locomotor behavior. Additionally, locomotion can be elicited by stimulation of the pontine locomotor region (PLR) (Mori et al., 1977) and the pyramidal tract in the medulla in mesencephalic cats (Shik et al., 1968).

Once higher-order brain locomotor centers become active, it is thought that they activate RS neurons, which then activate spinal CPGs. Anatomical studies have shown that the MLR, the SLR, and the fastigial nucleus all project to the medial reticular formation and activate a large population of RS neurons (Waller, 1940; Orlovsky, 1969; Orlovsky, 1970; Garcia-Rill et al., 1983; Steeves and Jordan, 1984; Baev et al., 1988; Mori et al., 1998). Also, during MLR-evoked locomotion in cats, reversible cooling of the medial reticular nuclei blocked evoked locomotion (Shefchyk et al., 1984). Additionally, fictive locomotion can be initiated by stimulation of RS neurons in the pontomedullary reticular formation in decerebrate birds (Steeves et al., 1987). Stimulation of descending RS neuron axons in the ventrolateral funiculus (VLF) in neonatal rats initiates locomotion (Cheng and Magnuson, 2011), and bilateral lesions of the VLF prevents activation of spinal CPGs, and therefore abolishes locomotor activity (Eidelberg et al., 1981).

Organization of Locomotor Command Systems in Lampreys

Despite having diverged from the lineage of higher vertebrates ~500 million years ago (Smith et al., 2013), the lamprey has a CNS that shares many basic neuroanatomical and functional similarities with those of higher vertebrates, such as a locomotor system consisting of higher-order brain locomotor centers, RS neurons, and spinal CPGs (Fig. 1). For the lamprey, microstimulation of the following brain regions can initiate spinal locomotor activity: (a) mesencephalic locomotor region (MLR) (Sirota et al., 2000; reviewed in Dubuc et al., 2008); (b) diencephalic locomotor region (DLR) (El Manira et al., 1997, reviewed in Dubuc et al., 2008); and (c) rostrolateral rhombencephalon (RLR), the dorsolateral mesencephalon (DLM), and the ventromedial diencephalon (VMD) (Paggett et al., 2004; Jackson et al., 2007). Several of these brain locomotor command regions project to and activate RS neurons located in the anterior (ARRN), middle (MRRN), and posterior (PRRN) rhombencephalic reticular nuclei (Fig. 2) (Paggett et al., 2004).

Small lamprey RS neurons are both necessary and sufficient for generation of locomotion. For example, lesioning the lateral tracts of the spinal cord, which contain most of the descending axons of small RS neurons, abolishes locomotion (Shaw et al., 2010). Additionally, microstimulation in parts of the ARRN, MRRN, and PRRN in the brain is sufficient to generate spinal locomotor activity (Jackson et al., 2007), while blocking activity in these nuclei can reduce or inhibit spinal locomotor activity initiated from higher-order brain centers (Paggett et al., 2004). In addition to being necessary and sufficient for initiation of locomotion, small RS neurons are rhythmically active during

fictive locomotion (Kasicki and Grillner, 1986; Kasicki et al., 1989). As in higher vertebrates, RS neurons in the lamprey project to all levels of the spinal cord (Davis and McClellan, 1994b) and activate spinal CPGs by releasing excitatory amino acids (EAA), such as glutamate (Buchanan et al., 1987). Application of EAAs or their agonists to the spinal cord activates spinal CPGs and elicits "fictive" locomotion (reviewed in Grillner and Wallén, 1999).

For several experimental reasons, most electrophysiological recordings from lamprey RS neurons are made from large, identified RS neurons called Müller cells (Fig. 2) (Rovainen, 1978). The cell bodies of Müller cells are substantially larger than most other RS neurons, and as such provide for stable intracellular recordings. Additionally, Müller cells are identified, which allows comparisons of the biophysical properties of the same neurons between brains. Finally, Müller cells are bilaterally symmetrical and have ipsilateral descending axons, and this allows neurons in one side of the brain to be manipulated in some way (e.g. injured), and then directly compared to control neurons (e.g. uninjured) on the other side of the brain.

Although Müller cells are good candidates for electrophysiological recordings, there is some uncertainty whether these neurons are locomotor command neurons that activate spinal CPGs and contribute to initiation of locomotion. On the one hand, Müller cells are neither necessary nor sufficient for initiation of locomotion. For instance, severing the medial tracts of the spinal cord, which contain most of the descending axons of Müller cells, does not abolish spinal locomotor activity (Shaw et al., 2010). Additionally, stimulation of the anterior MRRN, which contains several of the Müller cells, does not elicit spinal locomotor activity (Jackson et al., 2007). On the other hand,

Müller cells are rhythmically active during locomotion (Kasicki and Grillner, 1986; Kasicki et al., 1989; Deliagina et al., 2000; Zelenin, 2005), similar to small RS neurons. In addition, repetitive stimulation of these neurons during fictive locomotion can modulate burst frequency (Buchanan and Cohen, 1982), suggesting that Müller cells have direct or indirect inputs to spinal CPGs, similar to those of small, unidentified RS neurons. In addition, following spinal cord injury (SCI), Müller cells and unidentified RS neurons display similar "injury phenotypes" (McClellan et al., 2008), and like unidentified RS neurons, Müller cells are capable of axonal regeneration (Davis and McClellan, 1994a,b).

Spinal Cord Injury in Higher Vertebrates

For higher vertebrates, including humans, severe spinal cord injury (SCI) damages the descending axons of RS neurons and causes loss of locomotor function below the lesion. Because RS neurons of higher vertebrates are normally unable to regenerate their descending axons through the spinal lesion site, paralysis usually is permanent (Schwab and Bartholdi, 1996). For humans, it is estimated that worldwide, between 250,000 to 500,000 people suffer SCIs every year (World Health Organization. WHO.int). Despite advancements in medicine and research, at present there is no cure for SCI, and thus it is critical to understand the neural changes that occur within the locomotor system following SCI to better treat these injuries.

The inability of injured axons to regenerate in the CNS of mature, higher vertebrates is due to several factors: (a) myelin-associated inhibitory proteins (i.e. Nogo, MAG, and OMgp) (reviewed in Hunt et al., 2002; Schwab, 2004); (b) secondary injury effects, such as inflammation and hemorrhagic necrosis (Beattie et al., 2002; Whalley et al., 2006); (c) release of neurotoxic agents (Schwab and Bartholdi, 1996); and (d)

development of glial scar tissue that creates a physical as well as a chemical barrier for axonal regeneration (Silver and Miller, 2004; Silver et al., 2009). For these reasons, following SCI, any regenerative response mounted by injured RS neurons is halted, and locomotor function does not recover below the spinal cord lesion site.

Spinal Cord Injury in Lower Vertebrates

In contrast to mature higher vertebrates, following SCI in certain lower vertebrates, such as amphibians (Davis et al., 1990), fish (Becker et al., 1997), and lampreys (Davis and McClellan, 1994a,b), RS neurons display robust axonal regeneration through the injury site, and locomotor behavior recovers in a few weeks. Lower vertebrates display this remarkable ability for several reasons: (a) the CNS of lower vertebrates is a permissive environment for axonal regeneration and possess the necessary cues for directed axonal regeneration and synaptogenesis (Holder and Clarke, 1988; Taylor et al., 1989); (b) some lower vertebrates lack myelin (lamprey), while other have insufficient amounts of myelin-associated inhibitory proteins to prevent axonal regeneration (reviewed in McClellan, 1998); (c) lower vertebrates are cold blooded, and therefore have comparatively low metabolisms and oxygen needs, making them resistant to secondary injury effects, such as anoxia from disruption of blood flow following SCI (reviewed in Bicker and Buck, 2007; Wilkie, 2011); and (d) the glial scar is minimal and does not form an impenetrable barrier following SCI (Lurie and Selzer, 1991). Thus, the CNS of lower vertebrates is permissive for axonal regeneration, and as such these organisms make excellent SCI model systems to investigate the cellular and molecular mechanisms for functional axonal regeneration and recovery of function.

Behavior Recovery after Spinal Cord Injury for Lampreys

As previously mentioned, lampreys have a CNS that shares many basic neuroanatomical and functional similarities with those of higher vertebrates, but displays robust axonal regeneration following severe SCI. For example, following a complete transection of the rostral spinal cord, the injured descending axons of RS neurons spontaneously regenerate through the healed lesion site and make functional synapses, thereby restoring virtually normal behavior within ~8 weeks (Davis et al., 1993; Davis and McClellan, 1994a,b). For normal lampreys, RS neurons project their axons to all levels of the spinal cord (Davis and McClellan, 1994a,b), but interestingly, following SCI and subsequent restoration of locomotion, most RS neurons regenerate their axons for relatively short distances below the healed SCI site (Davis and McClellan, 1994a,b). Results from previous studies have suggested that descending propriospinal (PS) neurons are a possible compensatory mechanism that allows relatively complete recovery of locomotion despite incomplete axonal regeneration (Rouse and McClellan, 1997; Benthall et al., 2017). Although injured RS neurons only regenerate their axons for relatively short distances below the spinal lesion site, they display a robust regenerative response, and thus it is important to study the cellular conditions that support this regeneration.

Biophysical Changes for Lamprey RS Neurons Following SCI

To better understand some of the mechanisms that allow axonal regeneration and behavioral recovery of lampreys following SCI, recent studies have determined some of the changes in electrical and molecular properties that occur for injured RS neurons during the period of axonal regeneration. Understanding the changes in these properties following injury might potentially give clues as to the cellular conditions necessary to

support axonal regeneration.

Following SCI for the lamprey, injured RS neurons undergo a number of substantial changes in biophysical properties compared to those for uninjured neurons. For normal, uninjured RS neurons, the action potential (AP) is followed by three sequential after-potentials (McClellan et al., 2008): (a) fast afterhyperpolarization (fAHP) mediated by potassium channels; (b) afterdepolarization (ADP) that is not mediated by calcium channels but might depend on slow or persistent sodium channels; and (c) slow afterhyperpolarization (sAHP) mediated by influx of calcium via high-voltage activated (HVA) calcium channels that activates calcium-activated potassium (SK) channels. Additionally, for uninjured RS neurons, supra-threshold current pulses elicit a smooth train of APs that begin with a relatively high frequency and undergo moderate spike frequency adaptation (SFA) as firing frequency reaches a steady state. Studies of uninjured lamprey spinal neurons have shown that SFA is mediated by HVA calcium and SK channels (El Manira et al., 1994). For uninjured RS neurons, increasing the amplitude of the depolarizing current pulse results in a higher initial and steady state frequency of APs (Rouse et al., 1998).

At 2-3 weeks following SCI, injured lamprey RS neurons display several changes in biophysical properties that collectively are referred to as the "injury phenotype". First, injured RS neurons display significant changes for the afterpotentials compared to those for uninjured neurons (McClellan et al., 2008): (a) significant increase in the fAHP; and (b) the ADP and sAHP are significantly smaller or often are missing. Second, the repetitive firing patterns for injured RS neurons are substantially different than those for uninjured neurons. For example, uninjured RS neurons fire a smooth train of action

potentials in response to supra-threshold current pulses, while injured neurons fire several short bursts of APs or one short burst that terminates before the end of the current pulse (McClellan et al., 2008). Third, injured RS neurons often display several cycles of low amplitude, relatively high frequency (~20 Hz) membrane potential oscillations referred to as resonance (McClellan 2003,2009). For injured RS neurons that fire multiple short bursts, spontaneous resonance between bursts increases in amplitude and appears to trigger the subsequent burst. Injured neurons that fire a single, short burst usually do not display spontaneous resonance, but resonance can be triggered by membrane potential perturbations and decreases in amplitude. Also, resonance can be abolished by blockers for voltage-gated sodium channels (McClellan 2003,2009). At relatively long recovery times (~12-16 weeks) following SCI, regenerating axons of neurons make synapses below the spinal lesion site (Mackler and Selzer, 1987), and the electrical properties of most RS neurons are restored to normal (McClellan et al., 2008). At present, the changes in ion channels that mediate the altered biophysical properties are not fully understood.

It is thought that development of the "injury phenotype" following SCI is stimulated, in part, by disruption of target-derived neurotrophic factors from spinal neurons. For example, rostral SCI, which disrupts most synapses of RS neurons, triggers the injury phenotype and is a strong stimulus for axonal regeneration. In contrast, caudal SCI, which spares many of the synapses of RS neurons, usually does not trigger the injury phenotype and is a weak stimulus for axonal regeneration (Benes et al., 2017). Interestingly, following rostral SCI and after injured RS neurons regenerate their descending axons through the healed lesion site and make synapses with spinal targets, axonal regeneration is suppressed and normal biophysical properties are restored

(McClellan et al., 2008). Furthermore, for lampreys with SCI that recover at cold temperatures (~4-5^{o}C), RS neurons fail to develop the injury phenotype and do not regenerate their axons (Benes et al., 2017), possibly because retrogradely transported neurotrophic factors persist in the soma, and signal to the neuron that the spinal synapses are still intact. Also, pharmacological disruption of axonal transport can induce the injury phenotype for *uninjured* RS neurons (Pale, 2015).

Calcium Influx Hypothesis

The above changes in biophysical properties for injured lamprey RS neurons following SCI presumably establish an intracellular environment that is supportive for axonal regeneration. Of particular interest are changes in biophysical properties that minimize calcium influx for injured RS neurons. Recent studies have shown that for lamprey RS neurons in culture, focal depolarization of neurites or neuronal cell bodies with high potassium media or glutamate, both of which induce calcium influx, cause collapse of the growth cone and inhibition of outgrowth (Ryan et al., 2007). Similarly, increasing intracellular calcium levels inhibits neurite outgrowth for rat sensory neurons (Al-Mohanna et al., 1992). Furthermore, contact of neurites of mammalian neurons in culture with mature myelin and myelin-associated inhibitory proteins, such as Nogo, triggers calcium influx and growth cone collapse (reviewed in Schwab 2004), which can be blocked by calcium channel blockers (Moorman and Hume, 1993; Bandtlow et al., 1993). Also, following SCI, the central, ascending axons of rat dorsal root ganglion (DRG) neurons are able to regenerate if their peripheral axonal branch has received a pre-conditioning axotomy, which abolishes neuronal activity and down-regulates Cav1.2 channels (Enes et al., 2010). Together these results suggest that for many neurons that

are regenerating their axons, calcium influx is detrimental and can cause growth cones to stop advancing, and even collapse. For lamprey RS neurons, maintaining relatively low intracellular calcium levels and/or preventing large increases in internal calcium levels are potentially important conditions for successful axonal regeneration.

There are several potential mechanisms by which injured lamprey RS neurons could minimize calcium influx and maintain relatively low intracellular calcium levels. First, at early recovery times following SCI when injured RS neurons display the "injury phenotype", there is a significant decrease in mRNA expression of and down-regulation of both HVA calcium and SK channels (McClellan et al., 2008). The down-regulation of these channels appears to mediate the significant reduction or elimination of the sAHP, which is mediated in part by HVA calcium channels (McClellan et al., 2008).

Second, injured RS neurons undergo changes to many passive electrical properties that reduce the neuron excitability and calcium influx. For example, injured neurons display a more depolarized AP threshold (V_{th}) as well as a decrease in input resistance (R_{in}) (reviewed in McClellan, 2013). Together, these altered passive properties cause injured RS neurons to require more depolarizing current to fire APs, thus reducing the excitability of the neurons and limiting calcium influx.

Third, there a number of other potential changes in biophysical properties of injured RS neurons that could reduce calcium influx and maintain relatively low internal calcium levels. For example, outward rectifying potassium channels have been shown to reduce membrane excitability, which decreases calcium influx for the growth cones of chick spinal commissural neuron, as well as in rat callosal axons (Huang et al., 2017). For the lamprey, outward rectifying potassium channels are present in spinal dorsal cells

(Parker and Grillner, 1996), but the possible contribution of these channel to the injury phenotype for RS neurons has not been tested.

Focus of the Current Study

For the present study, current clamp and voltage clamp intracellular (IC) recordings were made from uninjured and injured lamprey RS neurons to determine the biophysical changes that occur following SCI, and to better understand the underlying mechanisms that mediate these changes. First, a delayed outward rectifying potassium current was compared for uninjured and injured RS neurons, and the possible increase of this current for reducing excitability of injured RS neurons was tested.

Second, pharmacological experiments were performed to test if partially blocking voltage-gated sodium channels might induce components of the "injury phenotype" for *uninjured* RS neurons. For example, it was found that injured RS neurons displayed a larger fAHP and a higher slope for repolarization following APs, as well as a larger AP amplitude. These results suggested that both potassium and sodium conductances increase for injured neurons, but perhaps with a larger increase for K^+ channels. Thus, if there is a differential increase in conductance for both of these channels (i.e. $\Delta g_K > \Delta g_{Na}$), we hypothesize that partially blocking Na+ channels for *uninjured* RS neurons might mimic this condition and induce an injury-like phenotype, such as irregular repetitive firing patterns and membrane resonance. Results from these experiments might elucidate some of the ion channel changes that occur in response to SCI and that mediate the altered biophysical properties of injured RS neuron.

Because lampreys demonstrate robust axonal regeneration and behavioral recovery following SCI, determining the neuronal changes that occur for RS neurons

following injury is important for understanding the cellular and molecular conditions that support successful axonal outgrowth. This and other information might provide insights for developing therapies and treatments for SCI in higher vertebrates, including perhaps humans.

Figure 1. Simplified model of the locomotor system in the lamprey. Brain command systems are comprised of higher-order centers that activate reticulospinal (RS) neurons. The RS neurons transmit descending neural commands for locomotion into the spinal cord and activate central pattern generators (CPGs), which are neural networks intrinsically capable of generating rhythmic locomotor activity for activating various body muscles in the proper temporal sequence.

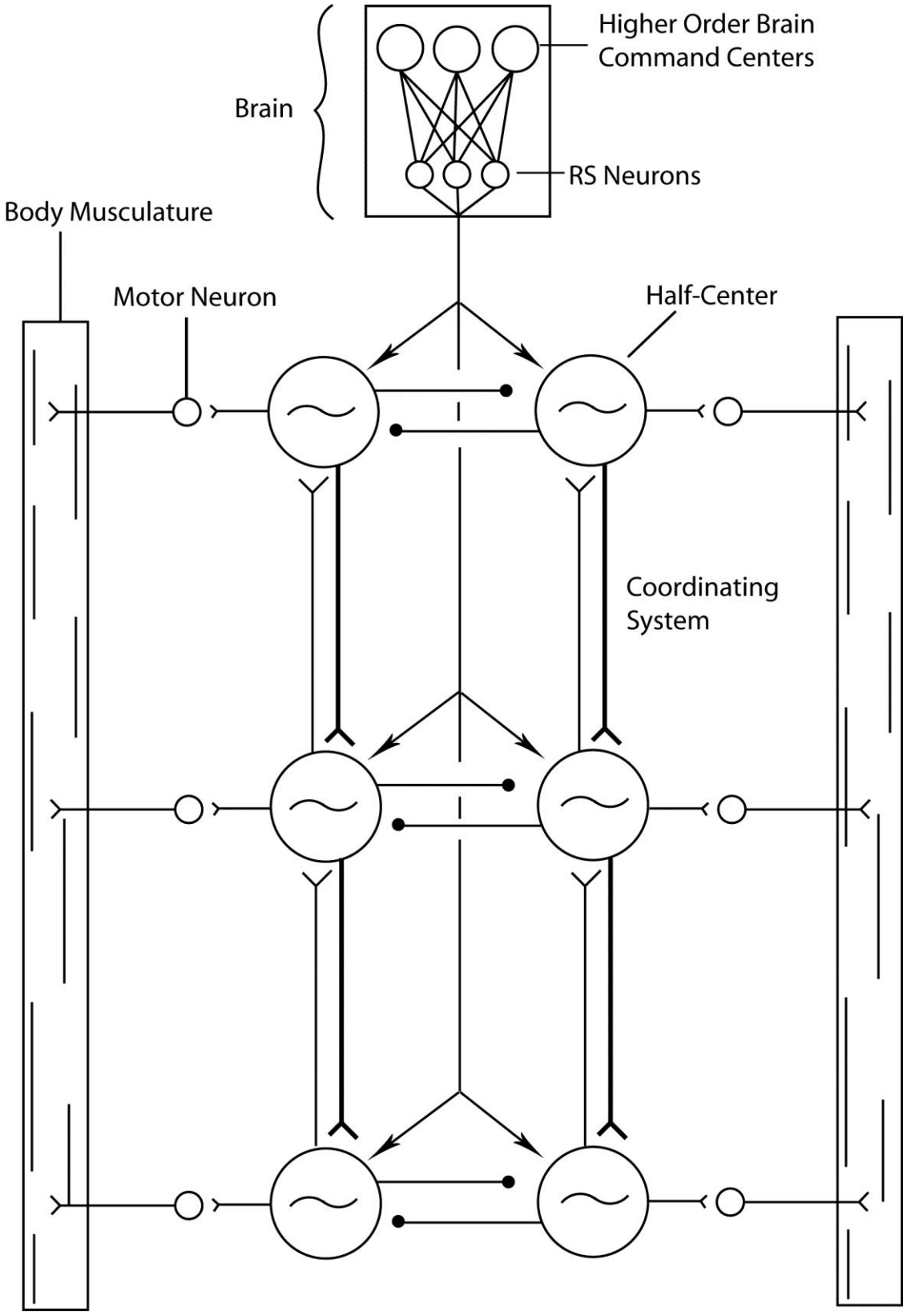
Higher Order Brain
Command Centers
Brain
RS Neurons
Body Musculature
Motor Neuron
Half-Center
Coordinating
System

Figure 2. Dorsal surface of the brain of a larval lamprey (~2 mm wide, depending on the size of the animal). (top) Upper half of figure is an image of the right dorsal surface of the lamprey brain, and the lower half is a diagram of the left side of brain. Contours represent the four reticular nuclei: mesencephalic reticular nuclei (MRN); anterior rhombencephalic reticular nuclei (ARRN); middle rhombencephalic reticular nuclei (MRRN); and posterior rhombencephalic reticular nuclei (PRRN). Each half of the lamprey brain contains 14 large, identified RS neurons called Müller cells and Mauthner cells (dots). (lower) Enlargement of reticular nuclei showing Müller and Mauthner cells (dots – not to scale). Müller cells: M cells (M1, M2, and M3) located in MRN; I cells (I1, I2, I3, and I4) located in ARRN; and B cells (B1, B2, B3, B4, and B5) located in MRRN. Mauthner (Mau) and axillary Mauthner (AM) cells are located in the MRRN. All reticular nuclei, including the PRRN, contain small, unidentified RS neurons (omitted for simplicity). Müller cells have ipsilateral descending axons, while Mauthner cells have contralaterally projecting descending axons.

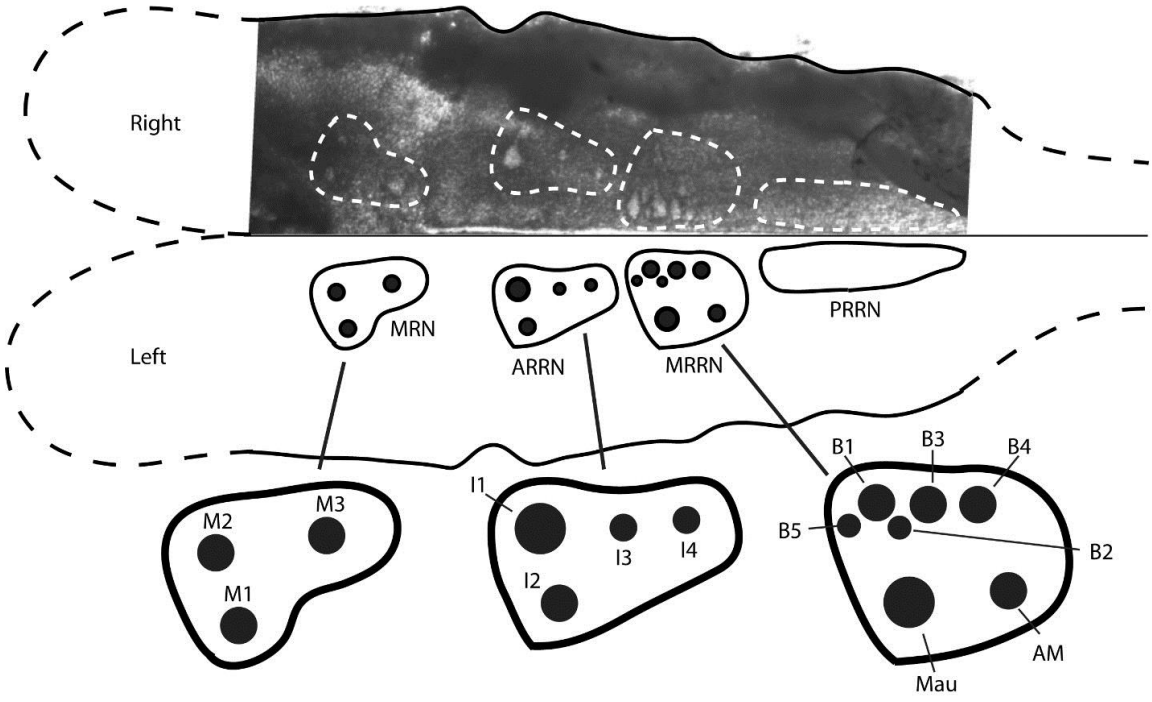
Right
Left
MRN
ARRN
MRRN
PRRN
M1
M2
M3
I1
I2
I3
I4
B1
B2
B3
B4
B5
AM
Mau

METHODS

Animal Care

Larval sea lampreys (*Petromyzon marinus*, n = 123 animals, ~100-140 mm) were used for all studies and were maintained in ~10 liter aquaria at 23-25°C. The Animal Use and Care Committee at the University of Missouri has approved the procedures in this study.

Spinal Cord Lesions

To compare the electrical properties of injured and uninjured lamprey RS neurons, three animal groups were used: (a) normal animals with no spinal lesions (n = 77 animals) (Fig. 3A); (b) experimental animals with right spinal hemi-transections (HTs) at 10% body length (BL, normalized distance from the anterior tip of the oral hood) that selectively injured the ipsilaterally projecting, descending axons of large, identified RS neurons on the right side of the brain, while leaving neurons on the left side uninjured (n = 30) (Fig. 3B); and (c) experimental animals with left-right double spinal HTs at 10% BL that injured all of the descending axons of RS neurons (n = 16) (Fig. 3C). Animals with right HTs were used to compare injured and uninjured RS neurons in the same brain. Animals with double HTs were used to increase the yield of injured RS neurons and to ensure that neurons were in fact injured when the injury status could not be determined (e.g. TTX in bath). Experimental animals were first anesthetized in tricaine methanesulfonate (MS222, ~100 mg/ 200 ml; Sigma Chemical Co., St. Louis, MO), and a 5 mm incision was made at 10% BL along the dorsal midline to expose the spinal cord. The meninges covering the dorsal surface of the spinal cord were temporarily deflected, and fine forceps were used to lesion the cord. The meninges were repositioned over the

injury, and the incision was closed. Following surgery, animals were placed in their home aquaria to recover for 2-3 weeks, at which time the changes in electrical properties of injured RS neurons are maximal (McClellan et al. 2008).

Isolated Brain-Spinal Cord Preparation

Dissection. Normal animals, or experimental animals that had recovered for 2-3 weeks, were anesthetized, and the brains and rostral spinal cords were exposed in cold, oxygenated lamprey Ringer's solution (10 mM HEPES, 130 mM NaCl, 2.1 mM KCl, 2.6 mM $CaCl_2$, 1.8 mM $MgCl_2$, and 4.0 mM Dextrose. pH = 7.4). The meninges were removed from the surface of the brain, and the cranial nerves and spinal roots were severed. The brain and rostral spinal cord were then removed from the carcass and pinned dorsal-side-up on a small strip of Sylgard (Corning Co; Midland, MI). Subsequently, the choroid plexus was removed, the cerebral commissure was cut, and the obex was extended caudally, as previously described (Davis and McClellan, 1994a). Finally, the brain was pinned flat, and the Sylgard strip was transferred to a recording chamber containing oxygenated lamprey Ringer's solution (6-8°C) (Fig. 3).

Recording set-up. Intracellular sharp micropipettes were pulled with a horizontal puller (Model P-80; Sutter Instruments, Novato, CA) from thin-walled glass (World Precision Instruments, Inc. Sarasota, FL). Microelectrodes were filled with 5 M potassium acetate, and then plugged into a holder containing 3 M potassium chloride. The electrode holder was inserted into either a x0.1L or x1.0L head-stage, which was connected to an intracellular amplifier (Axoclamp 2A; Axon Instruments, Foster City, CA). For recordings made in discontinuous current clamp mode (DCC; f_s = 2-6 kHz) and "bridge" mode, microelectrodes had resistances of ~50-70 MΩ, while for recordings

made using discontinuous single electrode voltage clamp (dSEVC; f_s = 2 kHz), microelectrode resistances were ~10-15 MΩ. A micromanipulator was used under manual control to position the tip of the micropipette near the surface of an RS neuron, and a dc motor was then used to rapidly advance the electrode in 1 μM increments until the cell was impaled. Immediately following penetration of an RS neuron, a small amount of hyperpolarizing current was applied to minimize spontaneous action potentials (i.e. injury discharge). After a few minutes, the membrane tightly sealed around the tip of the electrode, and the hyperpolarizing current was removed, leaving the neuron at its resting membrane potential (V_{rest}). For neurons to be included in the analysis, V_{rest} had to be more negative than -65 mV, and the peak of the action potential (AP) had to be more positive than +20 mV. However, many of the neurons had APs with amplitudes >100 mV (see Table 1).

For recordings made in the absence of tetrodotoxin (TTX), a suction electrode (SC) was placed around the caudal end of the spinal cord to record orthodromic action potentials elicited by RS neurons (Fig. 3). For *in vitro* preparations with lesioned spinal cords, the absence of orthodromic APs caudal to the spinal lesion site confirmed the injury status of an RS neuron. Intracellular recordings were stored on VHS tape (NeuroData DR890; Cygnus Technologies, Delaware Water Gap, PA; 11 kHz sampling frequency per channel), and also acquired with a custom data acquisition/analysis system (DT-3016 data acquisition board; Data Translations, Marlboro, MA).

Pharmacology

For some manipulations in the present study, the following ion channels blockers were used: (a) 0.5 mM kynurenic acid (KYN; Sigma Chemical Co., St. Louis, MO) –

blocks ionotropic excitatory amino acid receptors and reduces spontaneous electrical activity; (b) 3 μM tetrodotoxin citrate (TTX; Abcam, Cambridge, MA) – blocks voltage-gated sodium channels; (c) 150 pM TTX – partially blocks voltage-gated sodium channels; (d) 200 μM $CdCl_2$ and 400 μM $NiCl_2$ – blocks high-voltage activated (HVA) and low-voltage activated (LVA) calcium channels; (e) 10 mM tetraethylammonium chloride (TEA-Cl; Sigma) and 5 mM 4-aminopyridine (4-AP; Sigma) – partially blocks voltage-gated potassium channels; and (f) 1 μM UCL 1684 (Tocris Bioscience, Minneapolis, MN) – blocks calcium-activated potassium (SK) channels.

Intracellular Recording/Analysis

Action potential properties. Single APs were elicited for uninjured (N = 128) and injured (N = 84) RS neurons in the "bridge" mode by applying short depolarizing current pulses (+10 nA, 0.1-10 ms). The following biophysical properties were measured: (a) V_{rest} - resting membrane potential; (b) V_{AP} - the amplitude from V_{rest} to the peak of the AP; (c) dV_m/dt_{rise}, dV_m/dt_{fall} - the maximum slope of the rising and falling phases of the action potential, respectively; and (d) D_{AP} - the duration of the AP at half maximal amplitude.

Immediately following the main depolarizing phase of APs, uninjured RS neurons often displayed three sequential afterpotentials: (a) fAHP - fast afterhyperpolarization; (b) ADP - afterdepolarization; and (c) sAHP - slow afterhyperpolarization. Because of the small amplitudes of these afterpotentials, several AP sweeps were averaged, and the following parameters were measured (see N values in Table 1): (a) V - amplitude of an afterpotential component relative to V_{rest}; (b) d - delay from the peak of the AP to the peak of a given afterpotential; and (c) D – half-amplitude duration. If one of the

afterpotential components was clearly absent, the amplitude of that component was assigned a value of 0.0, and the other parameters of the component were marked as "not measurable". If an afterpotential component was present but not measureable (e.g. peak of ADP was hyperpolarized relative to V_{rest}), then all of the parameters for that component were marked as "not measurable".

Repetitive firing patterns. Threshold voltage (V_{th}) and repetitive firing patterns of uninjured (N = 113) and injured (N = 77) RS neurons were determined by applying depolarizing current pulses (0.01-10 nA, 2.0 s) using the DCC mode (f_s = 6 kHz). Uninjured RS neurons depolarized to V_{th} often responded with a single AP, and as such, V_{th} was measured as the steady state membrane potential following the AP. Injured RS neurons depolarized to V_{th} often responded with a short burst (or bursts) of APs, and therefore it was difficult to measure V_{th} under these conditions. Additionally, when depolarized near V_{th}, injured RS neurons often displayed a transient membrane depolarization followed by a delayed membrane repolarization (see Results). Therefore, for injured RS neurons, V_{th} was measured as the most depolarized membrane potential during a current pulse that was just sub-threshold for eliciting APs.

To elicit repetitive firing, supra-threshold depolarizing current pulses (0.01-10 nA, 2.0 s) were applied to uninjured and injured RS neurons. Repetitive firing patterns were characterized based on four possible phenotypes: (a) smooth train – spikes were elicited during the entire current pulse; (b) multiple bursts – several relatively short, consecutive bursts of APs; (c) single burst – brief, relatively high-frequency burst of APs at the beginning of the current pulse; and (d) single AP – one AP spike at the onset of the current pulse. Virtually all uninjured RS neurons fired a smooth train of APs, while

injured RS neurons could display one of the four firing patterns, and as such, the percentage of injured RS neurons with each firing pattern was determined. In addition to application of square current pulses, sine and triangle current waveforms (0.01-1.0 Hz) were applied to RS neurons to mimic the more physiological alternating excitatory and inhibitory synaptic inputs to these neurons that occur during locomotor activity (Kasicki et al. 1989).

At 2-3 weeks recovery times following SCI, many injured RS neurons in the lamprey, when depolarized to or above V_{th}, could display relatively high frequency (~20 Hz), low amplitude oscillations, referred to as "resonance" (McClellan 2003,2009). For injured RS neurons that displayed the multiple burst phenotype, membrane potential resonance between bursts increased in amplitude, and appeared to elicit the subsequent burst of APs. For injured RS neurons that fired a single burst of APs, membrane potential resonance was often present following termination of the burst, but the resonance decreased in amplitude and did not lead to subsequent bursts. For these particular injured RS neurons, membrane resonance could also be induced by brief perturbations of the membrane potential during the 2.0 s current pulse. Previous work has shown that blocking voltage-gated sodium channels with 3 μM TTX abolishes both spontaneous and induced membrane resonance (McClellan 2003,2009).

Passive electrical properties. In the DCC mode (f_s = 2 kHz), small, hyperpolarizing current pulses (0.01-3.0 nA, 0.2 s) were applied to elicit membrane hyperpolarization (ΔV_m) and to measure passive electrical properties of uninjured and injured RS neurons (see Table 1 for N values). Multiple voltage traces were averaged, and the membrane time constant was determined using two different methods: (a) double

exponential method (τ_m) (Golowasch et al. 2009); and (b) determining the 63% charging time (τ_{in}). For the double exponential method, membrane resistance (R_m) was calculated by dividing the change in membrane potential for the first exponential component by the applied current ($\Delta V0/I_m$), and then membrane capacitance ($C_m = \tau_m/R_m$) was calculated. For the 63% method, input resistance ($R_{in} = \Delta V_m/I_m$) and input capacitance ($C_{in} = \tau_{in}/R_{in}$) were calculated.

Delayed outward rectifying channel. As mentioned in the Introduction, outward rectifying potassium channels are activated by depolarization and then repolarize the membrane to reduce membrane excitability. For injured lamprey RS neurons, the possible role of a delayed outward rectifying potassium channel that might contribute to burst termination observed for two of the injury phenotypes (i.e. multiple bursts or single burst) was examined and compared to the properties for uninjured neurons.

First, for the DCC mode (f_s = 6 kHz), depolarizing current pulses (+0.01-10 nA, 2.0 s) were applied to uninjured (N = 113 neurons) and injured (N = 73) RS neurons. For injured RS neurons, application of depolarizing current pulses often elicited an initial transient membrane depolarization followed by a delayed repolarization to a steady state membrane potential. The amplitude of the delayed membrane repolarization was determined by measuring the difference in voltage from the peak of the initial transient depolarization to the steady state membrane potential at the end of the current pulse. Additionally, for the DCC mode (f_s = 2 kHz), symmetrical hyperpolarizing and depolarizing current pulses (±0.01-30 nA, 0.2-0.6 s) were applied to uninjured and injured neurons. The change in membrane potential (ΔV_m), in response to hyperpolarizing current, as well as from V_{rest} to the steady state membrane potential, was

used to construct V-I plots. To determine the linearity of the V-I plots, the average slopes ($R_{in} = \Delta V_m/\Delta I_m$) for membrane hyperpolarization were compared to the average slopes for membrane depolarization (unpaired t-test). If no significant difference was found, the membrane was classified as polarizing linearly. If R_{in} for depolarizing potentials was significantly less than R_{in} for hyperpolarizing potentials, the membrane was classified as polarizing non-linearly. The V-I plots were constructed to characterize the delayed repolarization for three different bath conditions: (a) without ion channel blockers – recordings from uninjured and injured RS neurons for membrane potentials up to V_{th} (uninjured: n = 29 animals, N = 73 neurons; injured: n = 26, N= 76); (b) TTX, $NiCl_2$, and $CdCl_2$ – recordings to determine parts of the V-I plot above V_{th} (uninjured: n = 3, N = 8; injured: n = 5, N = 5); and (c) TTX, $NiCl_2$, and $CdCl_2$ before and after applying TEA-Cl, and 4-AP – recordings to test if the delayed repolarization was mediated by a potassium channel (uninjured: n = 3, N = 3: injured: n = 5, N = 5).

Second, for the dSEVC mode (f_s = 2 kHz), RS neurons were held at V_{rest}, and voltage steps (± 1-30 mV, 0.2-0.6 s) were applied. For depolarizing voltage steps, delayed, outward rectification current was measured for both uninjured and injured RS neurons. Current recordings were made under three different bath conditions: (a) absence of ion channel blockers (uninjured: n = 4, N = 8; injured: n = 4, N = 7); (b) TTX, $NiCl_2$, and $CdCl_2$ (uninjured: n = 12, N = 23; injured: n = 9, N = 17); and (c) TTX, $NiCl_2$, and $CdCl_2$ before and after adding TEA-Cl and 4-AP (injured: n = 5, N = 5). For “a” and “b”, the passive leak currents were subtracted from the total measured currents, and the resultant current was assumed to be that of the outward rectifying potassium channel. For “c”, the total currents before and after adding TEA/4-AP were subtracted, and the

difference current was assumed to be that of the outward rectifier potassium channel.

From the dSEVC recordings, I-V plots were constructed and were used to estimate the effective activation voltage (V_K) of the delayed outward rectifying current. To estimate V_K, the slopes ($\Delta I_m/\Delta V_m$) between sequential points on the I-V plots were calculated and normalized to the largest slope, which occurred between the two right-most (most depolarized) points. The points that contributed to a normalized slope of ≥90% of the maximal slope were included in a linear regression, and the x-axis intercept was used to estimate V_K. For some RS neurons, the second largest slope was ≤90% of the maximum slope, and in these cases, only the two right-most points (maximum slope) were extrapolated to determine the x-axis intercept.

Effects of partial block of voltage-gated sodium channels. Membrane resonance displayed by injured RS neurons appears to involve voltage-gated sodium channels (McClellan 2003,2009). The data suggested that there was a differentially larger increase in g_K relative to g_{Na} for injured RS neurons compared to uninjured neurons (see Results). This differential condition for g_K and g_{Na} was mimicked by a weak, partial block of sodium channels for *uninjured* RS neurons to determine if the injury firing phenotype and membrane resonance could be induced. First, 3 μM TTX was added to the bath relatively far away from the brain (n = 7 animals, N = 7 neurons), and recordings were made from uninjured RS neurons at short time intervals to observe the effects of TTX as it gradually increased in concentration around the brain. Because the concentration of TTX eventually became high enough to completely block voltage-gated sodium channels, the window of time for a partial sodium channel blockage was ~5-10 min (starting at ~60 min). Second, to test the effects of a partial but continuous block of voltage-gated

sodium channels, various low dose concentrations of TTX were applied to *uninjured* RS neurons to determine a concentration (~150 pM TTX) that partially blocked voltage-gated sodium channels, but not did not abolish or substantially alter APs (n = 8, N = 25). Subsequently, experiments were performed in which 1 μM UCL 1684 and 150 pM TTX were applied to the bath of uninjured RS neurons (n = 6, N = 30) to block SK channels and partially block voltage-gated sodium channels, respectively. This combination of ion channel blockers was applied to mimic some of the biophysical changes that are thought to occur for injured RS neurons following injury (see Introduction).

Statistics. All data are presented as mean ± standard deviation (SD). The biophysical properties of uninjured and injured RS neurons were compared using either Mann-Whitney tests, or unpaired t-tests with Welch correction, when necessary (InStat; GraphPad Software, Inc., La Jolla, CA). Multiple data sets were compared using either a one-way ANOVA with Tukey-Kramer multiple comparisons post-test or a Kruskal-Wallis test with Dunn multiple comparisons post-test. Significance was assumed for $p \leq 0.05$.

Figure 3. Isolated lamprey brain-spinal cord preparations. (A) Diagram of brain and spinal cord from a normal animal showing intracellular micropipette for recording from uninjured RS neurons (open circles). (B) Diagram of brain and spinal cord showing right spinal hemi-transection (HT) at 10% body length (BL, normalized distance from anterior head) (vertical bar) that injures the right Müller cells (filled circle), without injuring the left Müller cells (open circle). (C) Diagram of brain and spinal cord showing double spinal HTs at 10% BL (vertical bars) that injure all Müller cells (filled circles). Intracellular (IC) micropipette for stimulating and recording electrical activity from the soma of RS neurons. Suction electrode (SC) for recording orthodromic APs from the spinal cord, caudal to the spinal lesion sites for B and C.

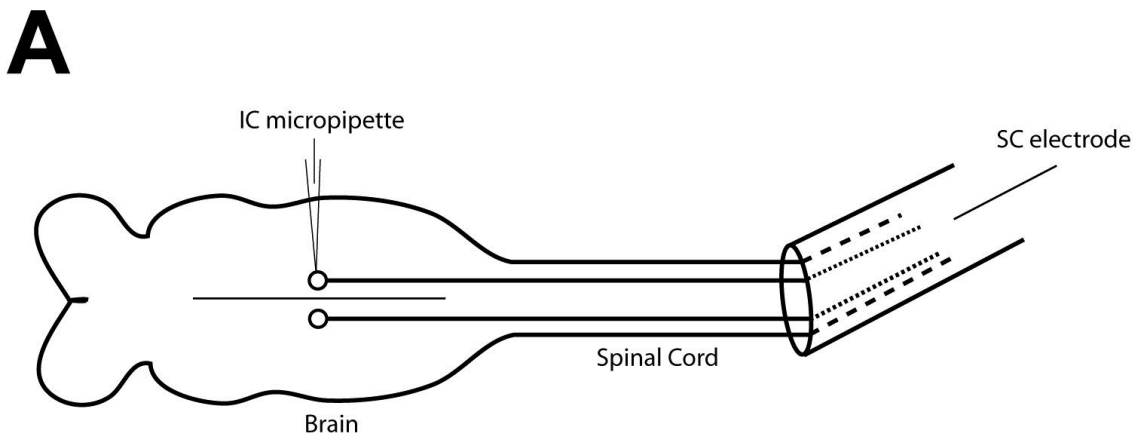
A
IC micropipette
SC electrode
Spinal Cord
Brain

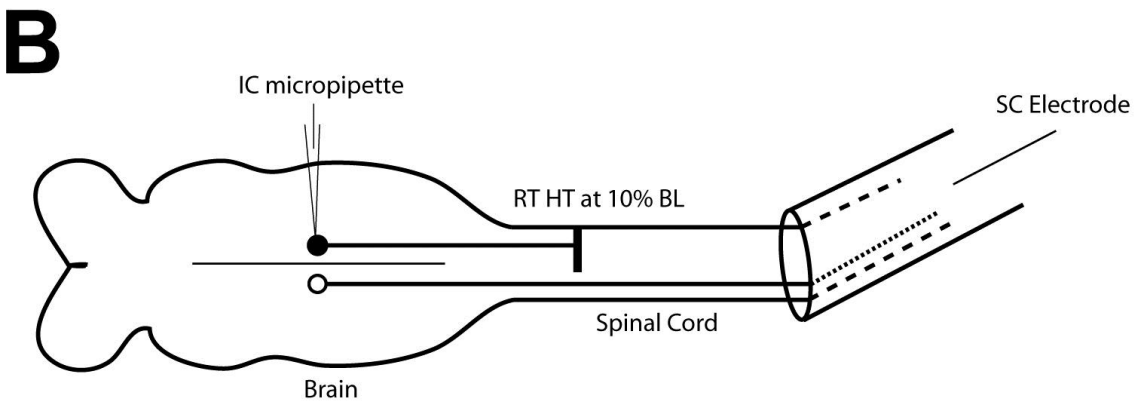
B
IC micropipette
SC Electrode
RT HT at 10% BL
Spinal Cord
Brain

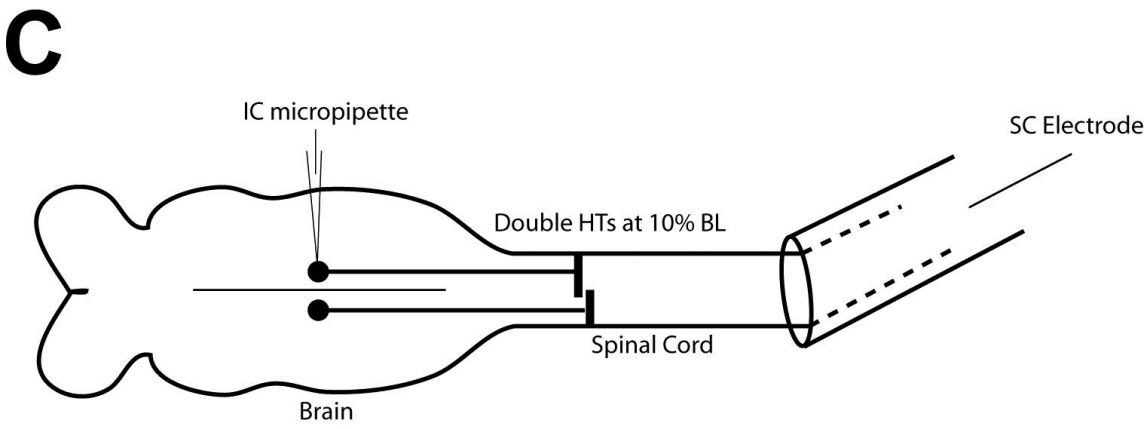
C
IC micropipette
SC Electrode
Double HTs at 10% BL
Spinal Cord
Brain

RESULTS

Biophysical Properties of Uninjured and Injured RS Neurons

Repetitive firing patterns. For normal, uninjured RS neurons, 98.2% (111/113) responded to supra-threshold current pulses by firing a smooth train of APs (Fig. 4A1,4A2). At 2-3 weeks after SCI, supra-threshold current pulses applied to injured RS neurons only elicited a smooth train of APs for 4.2% (3/72) of the neurons (shown below). Instead, 25.0% (18/72) of injured RS neurons displayed multiple bursts of APs (Fig. 4B1), 62.5% (45/72) displayed only a single burst of APs (Fig. 4B2), and 8.3% (6/72) only fired a single AP (shown below), regardless of the amount of depolarizing current (see Methods).

In addition to developing a new repetitive firing pattern, many injured RS neurons also displayed spontaneous membrane resonance, which was relatively high frequency (~15-20 Hz), low amplitude (~1-2 mV) oscillations of the membrane potential. For injured neurons that fired multiple bursts of APs, 100% (18/18) displayed several cycles of spontaneous membrane resonance that often increased in amplitude and appeared to generate the subsequent burst of APs (Fig. 4B1, inset). For neurons that fired a single burst of APs, only 8/45 displayed spontaneous membrane resonance, which decreased in amplitude with each oscillation cycle and did not generate subsequent bursts of APs (Fig. 4B2, inset). For the remaining 37/45 injured neurons that fired a single burst of APs, only one membrane oscillation was observed after the termination of the AP burst, and no spontaneous membrane resonance was seen for the remainder of the current pulse (Fig. 5C2). For all injured neurons that fired a smooth train of APs (3/3) as well as those that fired only a single AP (6/6), no spontaneous membrane resonance was observed. For

injured RS neurons that did not display spontaneous membrane resonance, brief perturbations of the membrane potential during the 2.0 s supra-threshold current pulse could induce membrane resonance that decreased in amplitude with time.

Action potential properties. Action potential (AP) properties of uninjured (N = 128 neurons) and injured (N = 84) RS neurons were recorded by applying short depolarizing current pulses (+10 nA, 0.1-10 ms) using the "bridge" mode. At 2-3 weeks following SCI, V_{rest} for uninjured and injured RS neurons was not significantly different (Table 1). Many of the other biophysical properties of RS neurons were significantly different following injury (Table 1): (a) significantly higher threshold potential (V_{th}) ($p \leq 0.001$); (b) significantly higher AP amplitude (V_{AP}) ($p \leq 0.001$); and (c) significantly greater slope for the repolarizing phase of the AP (dV_m/dt_{fall}) ($p \leq 0.01$) (unpaired t-tests with Welch correction when necessary). The slope for the depolarizing phase of the AP (dV_m/dt_{rise}) was greater but not significantly different ($p = 0.19$) for injured RS neurons compared to that for uninjured neurons.

Afterpotential properties. In addition to changes in the main depolarizing phase of APs, several changes occurred with regard to the afterpotential components that follow the AP, confirming previous reports (McClellan et al., 2008). For example, for uninjured RS neurons, the initial depolarization of the AP was followed by three sequential afterpotentials (Fig. 4A3): (a) fast afterhyperpolarization (fAHP); (b) afterdepolarization (ADP); and (c) slow afterhyperpolarization (sAHP). After SCI, injured RS neurons displayed a significantly larger fAHP ($p \leq 0.001$), and significantly smaller ADP ($p \leq 0.001$) and sAHP ($p \leq 0.001$) (Fig. 4B3) (Table 1).

Passive properties. Short, relatively small amplitude hyperpolarizing current

pulses (0.01-3.0 nA, 0.2 s) were applied to both uninjured (N = 118) and injured (N = 81) RS neurons to determine if the passive electrical properties of RS neurons changed following SCI. Several of the passive electrical properties did change following injury (Table 1): (a) significant decrease for both the membrane resistance (R_m) and the input resistance (R_{in}) ($p \leq 0.05$ and $p \leq 0.01$, respectively); (b) significantly longer membrane time constant (τ_m) and input time constant (τ_{in}) ($p \leq 0.05$ and $p \leq 0.001$, respectively); and (c) significantly greater membrane capacitance (C_m) and input capacitance (C_{in}) ($p \leq 0.01$ and $p \leq 0.001$, respectively).

For the above comparisons of biophysical properties, uninjured RS neurons were recorded from normal animals (no spinal lesions) (Fig. 3A), while injured neurons were recorded from animals with right spinal cord HTs at 10% BL (Fig. 3B). In particular it should be noted that "uninjured" RS neurons from animals with spinal HTs (i.e. orthodromic spinal AP) displayed significant lower values for R_{in} and R_m and significantly higher values for V_{th} and C_{in} compared to those for truly uninjured RS neurons from normal animals (ANOVA with Bonferroni multiple comparison post-test, or Kruskal-Wallis test with Dunn multiple comparison post-test.). Thus, presumed uninjured RS neurons in animals with spinal HTs might have responded in some minor way to the spinal lesion and not been truly uninjured. Alternatively, these differences might be attributable to the relatively low sample size for uninjured RS neurons from spinal HT-lesioned animals. Further investigation is required before a definitive conclusion can be drawn.

Transient Depolarization Followed by Delayed Repolarization

Effects of delayed repolarization on membrane potential. For many injured RS

neurons, but also some uninjured neurons, depolarizing current pulses near V_{th} elicited a transient membrane depolarization, followed by a delayed membrane repolarization (see Fig. 5). This was investigated using the DCC mode by applying depolarizing current pulses (0.01-10 nA, 2.0 s) to both uninjured (N = 113) and injured (N = 73) RS neurons. When depolarized to just sub-threshold, only 22.1% (25/113) of uninjured RS neurons displayed a delayed repolarization, and the average amplitude was -1.57 ± 0.92 mV (Fig. 5A1). In contrast, at sub-threshold membrane potentials, 97.3% (71/73) of injured RS neurons displayed a delayed membrane repolarization that had a significantly larger average amplitude (-6.36 ± 2.65 mV) compared to that for uninjured neurons (Fig. 5B1) ($p \leq 0.001$, unpaired t-test with Welch correction).

The transient membrane depolarization and delayed outward repolarization observed for most injured neurons and some uninjured neurons resisted or counteracted depolarization, causing the membrane potential to depolarize non-linearly as it approached V_{th} (Fig. 5B2). To quantify the linearity of the membrane potential polarization, V-I plots were made for uninjured (N = 73) and injured (N = 76) RS neurons in response to symmetrical hyperpolarizing and depolarizing current pulses (±0.01-30 nA, 0.2-0.6s). From these V-I plots, R_{in} (= $\Delta V_m/\Delta I_m$) values in response to hyperpolarizing current pulses were compared to R_{in} values in response to depolarizing current pulses, from V_{rest} to V_{th}. If the R_{in} values for depolarizing and hyperpolarizing current pulses were not significantly different, then the membrane potential was considered to polarize linearly, but if they were significantly different, then the membrane potential was classified as depolarizing non-linearly. For uninjured RS neurons, a significant percentage (49/73) displayed linear membrane polarization ($p \leq$

0.01) (Fig. 5A1,A2), while for injured RS neurons, a significant percentage (52/76) polarized non-linearly ($p \leq 0.01$; Sign test) (Fig. 5B1,B2). The delayed repolarization appeared to be more pronounced at sub-threshold membrane potentials for injured RS neurons as compared to uninjured neurons. Thus, injured RS neurons required significantly more membrane depolarization (N = 113 uninjured, N = 77 injured) (Fig. 6A) ($p \leq 0.001$, unpaired t-test) and more injected current (N = 110 uninjured, N = 79 injured) ($p \leq 0.001$, unpaired t-test with Welch correction) (Fig. 6B) to reach threshold compared to uninjured RS neurons. These changes in properties following SCI reduced excitability of injured RS neurons compared to that for uninjured neurons.

The effect of the delayed membrane repolarization at voltages depolarized to threshold for injured and uninjured RS neurons was recorded in the presence of blockers for voltage-gated sodium channels (3 μM TTX) and voltage-gated calcium channels (400 μM $NiCl_2$, and 200 μM $CdCl_2$). Under these conditions, an apparent non-linear region was revealed in the V-I plots for uninjured neurons at membrane potentials above V_{th}. (Fig. 5C). Applying the above analysis to the V-I plots indicated that if membrane potentials above V_{th} were included, 100% of both uninjured (8/8) and injured (2/2) RS neurons depolarized non-linearly (Fig. 5B2,C2).

To determine how the larger delayed repolarization for injured RS neurons affected the membrane potential in response to more physiological stimuli, sine and triangle current waveforms were applied to injured and uninjured RS neurons to simulate the phasic excitatory and inhibitory synaptic input these neurons receive during locomotion (Kasicki et al., 1989). For uninjured neurons (N = 78), triangle current injections appeared to result in relatively linear membrane hyperpolarization and

depolarization, and elicited a smooth train of APs when the membrane potential was depolarized above V_{th} (Fig. 7A). For application of triangle current to injured RS neurons (N = 50), the membrane potential appeared to polarize linearly in the hyperpolarizing direction. In contrast, in the depolarizing direction, between V_{rest} and V_{th}, the membrane potential clearly polarized non-linearly due to the delayed repolarization that resisted or counteracted further depolarization. For 19/50 injured RS neurons, the delayed repolarization was prominent enough to prevent the membrane potential from reaching V_{th} in response to ±10 nA triangle or sine current waveforms (Fig. 7B). For 27/50 neurons, the delayed repolarization still caused the membrane potential to depolarize non-linearly, but ±10 nA current waveforms were sufficient to reach V_{th} (Fig. 7C). The remaining 4/50 injured RS neurons could not be depolarized to V_{th} at lower frequency, ±10 nA sine and triangle current waveforms (<1 Hz), but at higher frequencies (≥1 Hz) apparently were able to overcame the delayed repolarization and fire APs.

To begin to identify the channels that might be activated to produce the delayed repolarization, recordings were initially made from uninjured and injured RS under conditions in which voltage-gated sodium channels and voltage-gate calcium channels were blocked (see Methods). As reported earlier, under these conditions all injured (5/5) and uninjured (8/8) neurons displayed a transient depolarization followed by a delayed repolarization, as well as non-linear depolarization at supra-threshold membrane potentials. These finding suggest that voltage-gated sodium and voltage-gated calcium channels do not contribute substantially to the delayed repolarization.

To separate the contribution of various voltage-gated ion channels to the delayed repolarization, continuous recordings were made from injured and uninjured RS neurons

first with no blockers added to the bath (Fig. 8A), subsequently in the presence of blockers for voltage-gated sodium and voltage-gated calcium channels (Fig. 8B), and finally after the addition of 10 mM TEA, and 5 mM 4-AP (N = 5 injured, N = 3 uninjured) (Fig. 8C). After application of potassium channel blockers to injured neurons, the amplitude of the delayed repolarization significantly decreased from -6.28 ± -2.14 mV to -1.48 ± -1.28 mV (N = 5 injured neurons) ($p \leq 0.01$, unpaired t-test). For uninjured neurons, these blockers reduced the amplitude of the delayed repolarization from -4.70 ± -1.88 mV to -0.55 ± -0.96 mV (N = 3 uninjured neurons). Thus, the delayed repolarization appears to be mediated by voltage-gated potassium channels.

Contribution of Delay Repolarization to Injury Phenotype

As previously reported, most uninjured RS neurons did not display a delayed repolarization, and fired a smooth train of APs in response to a 2.0 s supra-threshold depolarizing current pulse. At 2-3 weeks following SCI, most injured RS neurons displayed a delayed repolarization at sub-threshold membrane potentials, and also adopt the "injury phenotype", which includes changes in the repetitive firing patterns (see Fig. 4). Interestingly, components of the delayed repolarization, such as amplitude, delay to activation, and time course from the peak of the transient depolarization to V_m following the initial, rapid delayed repolarization (see # in inset for Fig. 9D1) appeared to correlate with the firing pattern displayed by a particular injured RS neuron (Table 2). For example, for the 4.2% (3/72) of injured RS neurons that fired a smooth train of APs (Fig. 9A2), only one neuron displayed a very small, delayed membrane repolarization, while the other two neurons displayed no detectable delayed membrane repolarization (Fig. 9A1). For 25.0% (18/72) of injured RS neurons, 2.0 s supra-threshold current pulses

elicited multiple bursts of APs and spontaneous membrane resonance (Fig. 9B2), and these neurons displayed a moderate delayed membrane repolarization (Fig. 9B1). For 62.5% (45/72) of injured neurons, 2.0 s supra-threshold current pulses elicited only a single burst of APs (Fig. 9C2), and only 8 of those neurons displayed spontaneous membrane resonance. These particular injured RS neurons displayed a significantly larger delayed membrane repolarization (Fig. 9C1) ($p \leq 0.01$), a shorter delay of activation ($p \leq 0.001$) and faster time course ($p \leq 0.01$) (one-way ANOVA with Tukey multiple comparisons post-test) than did the injured RS neurons that fired multiple bursts of APs (Table 2). The remaining 8.3% (6/72) of injured RS neurons displayed only a single AP in response to a depolarizing current pulses up to +10 nA (Fig. 9D2). For these particular neurons, the amplitude of the delayed repolarization was not significantly larger than those of neurons that fired a single burst of APs ($p = 0.113$), but the delay to activation and time course were both significantly shorter (Fig. 9D1) ($p \leq 0.01$, one-way ANOVA with Tukey multiple comparisons post- test) (Table 2).

Current Mediating Delayed Outward Repolarization

Delayed outward rectifying current. Voltage clamp recordings were made to characterize the current responsible for the delayed membrane repolarization. Initially, recordings were made from uninjured and injured RS neurons with no blockers for voltage-gated ion channels in the bath. At just sub-threshold membrane potentials (see horizontal dotted lines in Fig. 10C), uninjured lamprey RS neurons (N = 8) displayed an average current of -0.24 ± 0.25 nA, which was significantly less than the outward current of $+2.77 \pm 2.52$ nA displayed by injured neurons (N = 7) ($p \leq 0.05$, unpaired t-test with Welch correction) (Fig. 10). Due to the relatively low signal-to-noise ratio of the current

recordings, it was difficult to precisely quantify the time constant (τ) for the delayed outward rectifying current, but fitting the current traces with a single exponential curve yielded an approximate τ of ~20-30 ms.

The effective activation voltage of the repolarizing current for both uninjured and injured RS neurons (see Methods) was measured using voltage clamp in the presence of blockers for voltage-gated sodium and calcium channels (Fig. 11) (see Discussion). Under these conditions, V_{rest} was not significantly different for uninjured RS neurons (N = 23) compared to that for injured neurons (N = 17, unpaired t-test) (Fig. 12A). However, uninjured RS neurons displayed an effective activation voltage (V_K; see Methods) for the delayed outward rectifying current at significantly more depolarized voltages than for injured RS neurons ($p \leq 0.001$, unpaired t-test with Welch correction) (Fig. 11C,12B). Additionally, the total amount of membrane depolarization required to activate the outward current was significantly greater for uninjured neurons than for injured neurons ($p \leq 0.001$, unpaired t-test with Welch Correction) (Fig. 12C). To begin to reconcile if the activation voltage for this current was shifted, or if the conductance of the delayed outward channel was increased following injury, a scatter plot was constructed using I-V data points from 11 uninjured RS neurons and 6 injured RS neurons that had V_{rest} values within ~4 mV of each other (not shown). Each population was fit with a curve, and it was determined that scaling the currents of the I-V curve for uninjured RS neurons by a factor of ~4 resulted in a good fit to the I-V curve for injured neurons (e.g. see red line in Fig. 11C). This analysis, in addition to other evidence, such as an increase in the slope of the falling phase of the AP and an increase in the fAHP for injured RS neurons (see Discussion), suggests that the conductance of the outward rectifying channel was

increased following injury.

The pharmacology of the delayed outward rectifying current was determined by recording from injured RS neurons (N = 5) in the presence of 3 μM TTX, 400 μM $NiCl_2$, and 200 μM $CdCl_2$, before and after the addition of 10 mM TEA-Cl and 5 mM 4-AP. Under conditions in which voltage-gated potassium channels were blocked, scaling the outward current by an average factor of ~7.3 created a good fit with the current before addition of voltage-gated potassium blockers (dotted line in Fig. 13). Thus, the blockers reduced the amplitude of outward current to 13.7% ± 7.8% of the original current ($p \leq 0.001$, one-sample t-test) (Fig. 13). It should be noted that prior to blocking potassium channels, V_m could not be depolarized to the same level as after blocking these channels due to the large amplitude of the outward current and the limitations of dSEVC. Because TEA and 4-AP are broad-spectrum K^+ channel blockers that do not completely block voltage-gated potassium channels (Mathie et al., 1998; Magura et al., 2004; Roux 2005), the delayed outward rectifying current was significantly reduced, but not completely abolished in the presence of these blockers. In particular, for the example shown in Figure 13, scaling the current after application of K^+ channel blockers by 16 resulted in a good fit to the current before these blockers were applied (dotted line in Fig. 13).

Partial Block of Voltage-Gated Sodium Channels Induces Injury Phenotype

As reported above, there is a correlation between the amplitude of the delayed repolarization, which appears to be mediated by outward rectifying potassium channels, and the presence of membrane resonance (Fig. 9). In addition, membrane resonance can be abolished for injured RS neurons by blocking voltage-gated sodium channels (McClellan 2003,2009). As noted above, compared to uninjured RS neurons, for injured

neurons the fAHP and dV_m/dt_{fall} were both significantly larger, suggesting a relatively large increase in g_K, while V_{AP} was significantly larger but dV_m/dt_{rise} was not, suggesting a more moderate increase in g_{Na} (Table 1). Taken together, these results suggest that for injured RS neurons there might be a concurrent but differentially larger increase in the conductances of potassium channels relative to that for sodium channels, possibly due to a differential up-regulation of these channels. Experimentally, it is difficult to preferentially increase potassium currents, and therefore we hypothesized that membrane resonance might be induced for *uninjured RS neurons* by a relative decrease of inward current by partially blocking voltage-gated sodium channels.

Gradual block of voltage-gated sodium channels. For one experimental paradigm, 3 μM TTX was applied to one end of the bath away from the brain, and recordings were made from uninjured RS neurons (N = 7) at frequent intervals to observe the effects as the concentration of TTX gradually increased around the brain. Initially, uninjured neurons fired a smooth train of APs in response to a depolarizing current pulse (Fig. 14A), but after ~60 minutes, the concentration of TTX around the brain had apparently increased enough to begin to partially block some of the more TTX-sensitive voltage-gated sodium channel sub-types. At this point, the uninjured RS neurons began to fire multiple bursts of APs as well as spontaneous membrane resonance (Fig. 14B, see inset). After ~65 minutes, the firing pattern of uninjured RS neurons changed from multiple bursts of APs to a single burst of APs, which possible weak, short-duration resonance following the burst (Fig 14C, see inset). Finally, after ~70 minutes (10 minutes after initial effect of TTX), all APs were abolished.

Blocking SK channels and partially blocking voltage-gated sodium channels.

Because the window of time from the initial effects of 3 μM TTX to a complete block of electrical activity was brief, very few biophysical properties could be recorded for each experiment. To extend the time over which voltage-gated sodium channels were partially blocked, a low dose of TTX (~150 pM) was applied to the bath to partially block voltage-gated sodium channels but without blocking APs. With this concentration of TTX, 60.0% (15/25) of uninjured RS neurons converted from firing a smooth train of APs to multiple bursts of APs in response to a 2.0 s depolarizing current pulse, and 12.0% (3/25) transitioned from firing a smooth train of APs to a single burst of APs. The remaining 28.0% (7/25) of injured RS neurons continued to fire a smooth train of APs. Once this low dose concentration of TTX was determined that induced the injury phenotype for most uninjured RS neurons, experiments were performed in which SK channels also were blocked (1 μM UCL 1684) in addition to the partial block of voltage-gated sodium channels. This combination of blockers was applied to mimic some of the changes in ion channel expression that are thought to occur following SCI (McClellan et al., 2008). With this combination of blockers in the bath, 93.3% (28/30) of uninjured RS neurons transitioned from firing a smooth train of APs (Fig. 15A1) to firing multiple bursts of APs (15A2), and the majority of the neurons displayed membrane resonance (Fig. 15C, see inset). The remaining RS neurons (6.7%, 2/30) converted from firing a smooth train of APs (Fig. 15B1) to a single burst of APs with perhaps some weak, short-duration resonance following the burst (Fig. 15B2, see inset).

Figure 4. Repetitive firing and after-potentials for uninjured and injured left-right pairs of RS neurons at 2-3 weeks following right spinal cord hemi-transections (HTs) at 10% body length (BL, normalized distance from the anterior tip of the oral hood) (see Fig. 3B). Recordings of membrane potential (V_m) in response to 2.0 s current pulses (I_m) were made in the presence of 0.5 mM KYN. Freq = instantaneous firing frequency. (A1) Smooth train of APs for an uninjured I1 neuron on the left side of the brain, and (B1) multiple bursts of APs with membrane resonance (inset) for an injured I1 neuron on the right side. (A2) Smooth train of APs for an uninjured B3 neuron on the left side of the brain, and (B2) a single, short burst of APs for an injured B3 neuron on the right side with short resonance-like rebound following burst (inset). (A3) Uninjured I1 neuron with three sequential afterpotentials: fAHP; ADP; and sAHP (see text). (B3) Injured I1 neuron with only fAHP. Vertical/horizontal scale bars = (A1, B1, A2, B2) 60 mV, 10 nA, 30 Hz/0.65 s; (A3, B3) 4 mV/0.2 s. Insets enlarged by 3.0x.

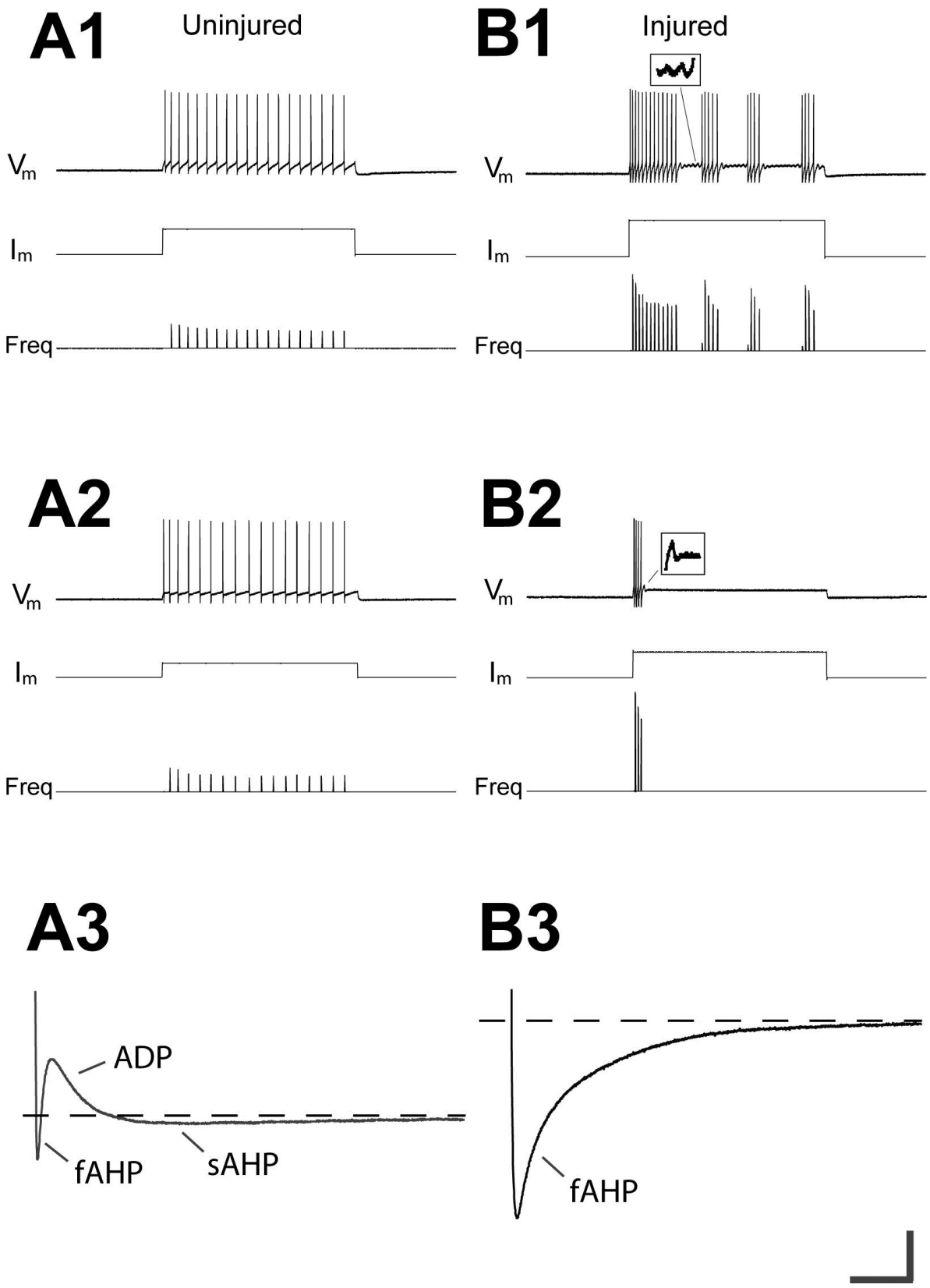
A1
Uninjured
B1
Injured
Vm
Im
Freq
A2
B2
A3
B3
ADP
fAHP
sAHP

Figure 5. Membrane potential (V_m) of uninjured and injured RS neurons in response to 0.2 s symmetrical hyperpolarizing and depolarizing current pulses (I_m). (A1) Response of an uninjured B1 neuron and (A2) the corresponding V-I plot showing relatively linear depolarization to V_{th} (horizontal dotted line). (B1) Response of an injured B1 neuron in the same brain and (B2) the corresponding V-I plot showing non-linear depolarization to V_{th} (horizontal dotted line). (C1) Response of an uninjured B1 neuron in the presence of 3 μM TTX, 400 μM $NiCl_2$, and 200 μM $CdCl_2$ and (C2) the corresponding V-I plot showing non-linear depolarization about V_{th}, which because of the presence of TTX was estimated from the average ΔV_m value above V_{rest} required to reach V_{th} for uninjured RS neurons (see Figure 6A). Dashed lines = linear extrapolation of initial membrane polarization. Vertical/horizontal scale bars = 20 mV, 5 nA/0.04 s. The APs are clipped for A1 and B1 (horizontal dashed lines).

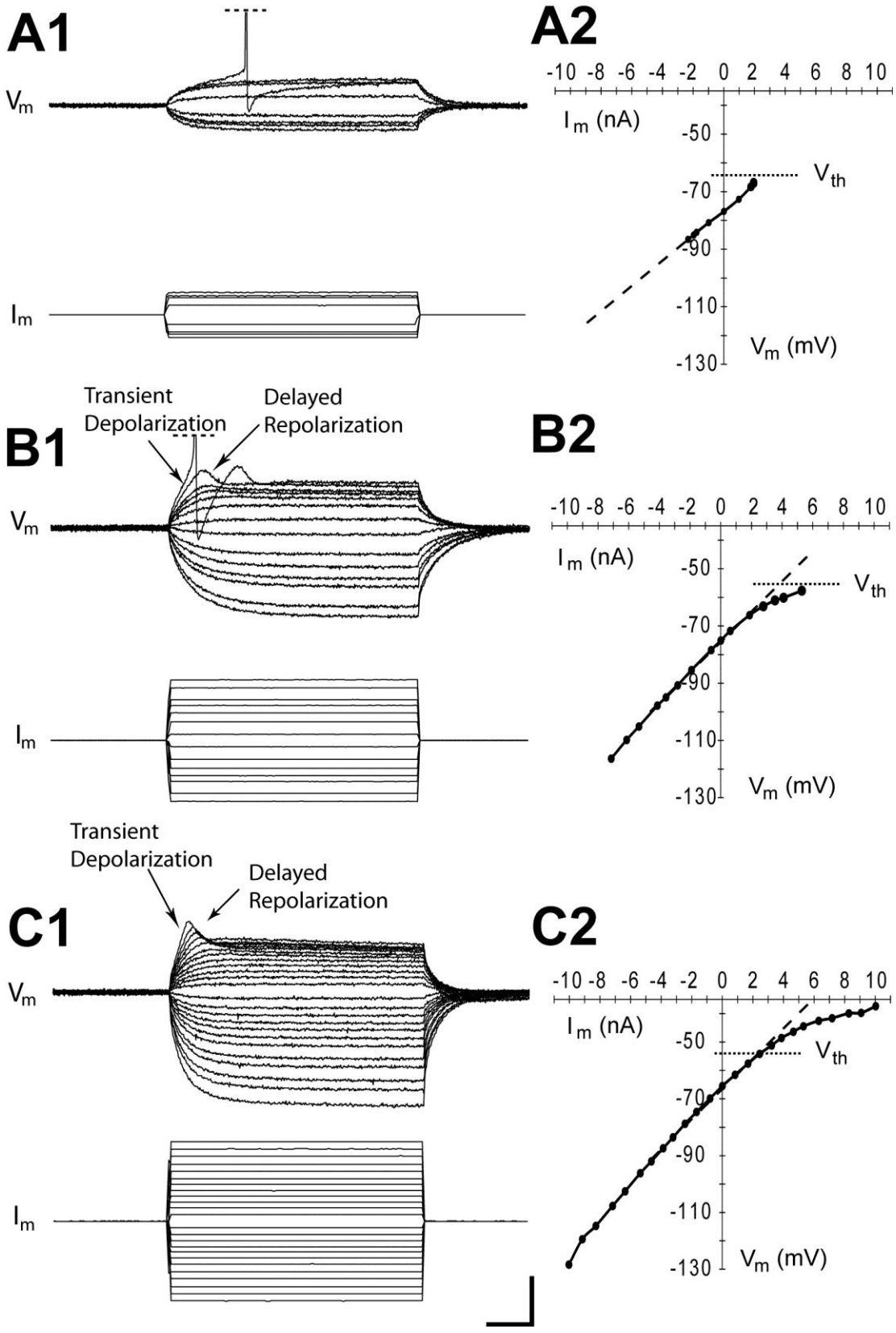
A1
Vm
Im
A2
-10 -8 -6 -4 -2 0 2 4 6 8 10
Im (nA)
-50
-70
-90
-110
-130
Vth
Vm (mV)
Transient Depolarization
Delayed Repolarization
B1
Vm
Im
B2
-10 -8 -6 -4 -2 0 2 4 6 8 10
Im (nA)
-50
-70
-90
-110
-130
Vth
Vm (mV)
Transient Depolarization
Delayed Repolarization
C1
Vm
Im
C2
-10 -8 -6 -4 -2 0 2 4 6 8 10
Im (nA)
-50
-70
-90
-110
-130
Vth
Vm (mV)

Figure 6. Histograms showing the change in membrane potential (ΔV_m) as well as the amplitude of depolarizing current (I_m) required for uninjured and injured RS neurons to reach V_{th}. (A) ΔV_m (V_{rest} to V_{th}) for uninjured RS neurons (N = 113) was significantly smaller than that for injured RS neurons (N = 77) (*** – $p < 0.001$, unpaired t-test). (B) Amplitude of depolarizing current required to reach V_{th} for uninjured neurons (N = 109) was significantly less than that for injured RS neurons (N = 79) (*** – $p < 0.001$, unpaired t-test with Welch correction).

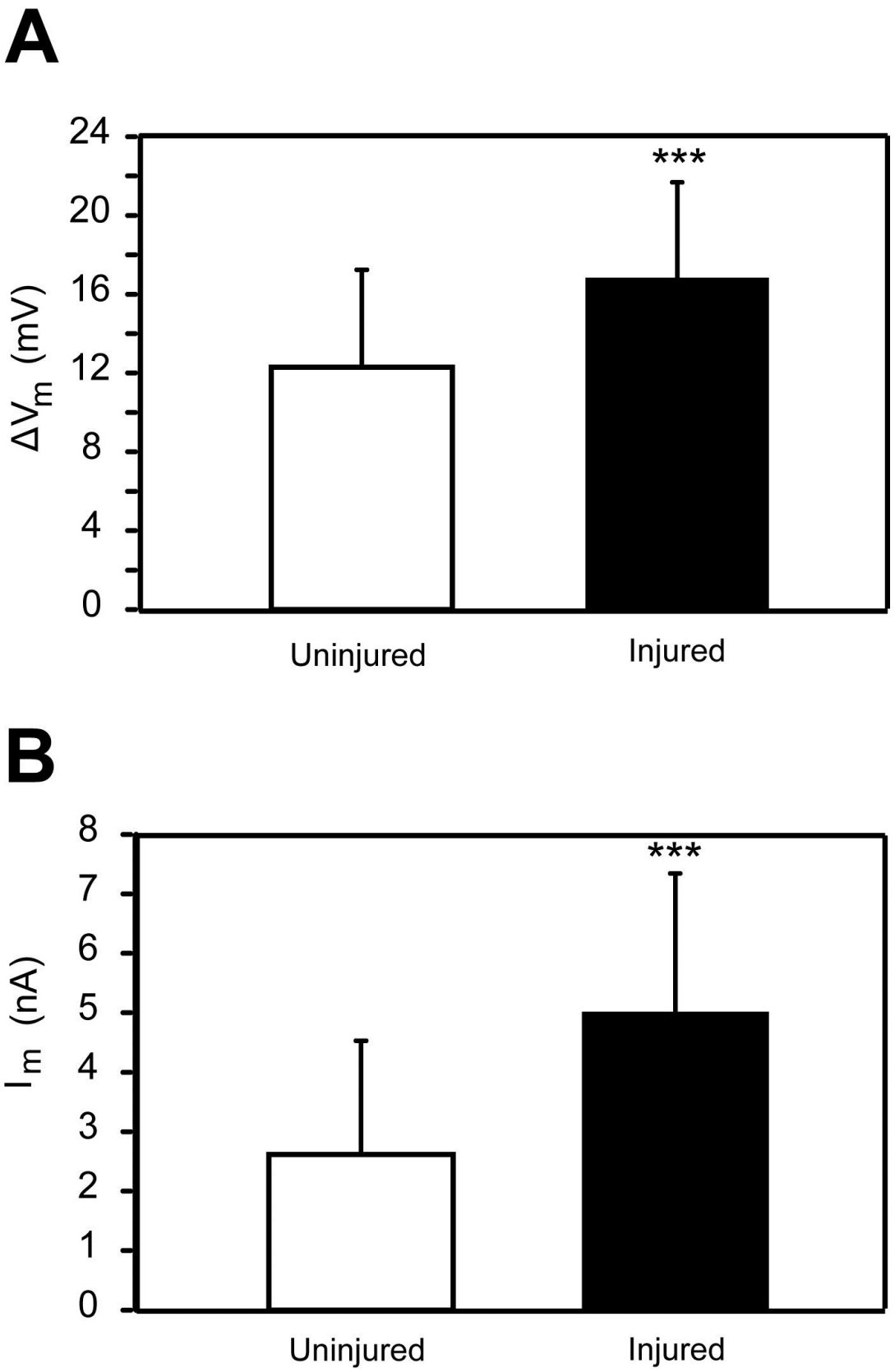
A
24
20
16
12
8
4
0
ΔVm (mV)
***
Uninjured
Injured
B
8
7
6
5
4
3
2
1
0
Im (nA)
***
Uninjured
Injured

Figure 7. Membrane potential (V_m) of uninjured and injured RS neurons in response to 0.5 Hz triangle current waveforms (I_m) in the presence of 0.5 mM KYN. Freq = instantaneous firing frequency. (A) Membrane polarization for an uninjured B1 neuron, and (B) an injured B1 neuron recorded from the same brain. (C) Membrane polarization for an injured I1 neuron. Dotted lines = linear extrapolation of initial membrane polarization. Vertical/horizontal scale bars = 20 mV, 5 nA, 12.5 Hz/0.5 s.

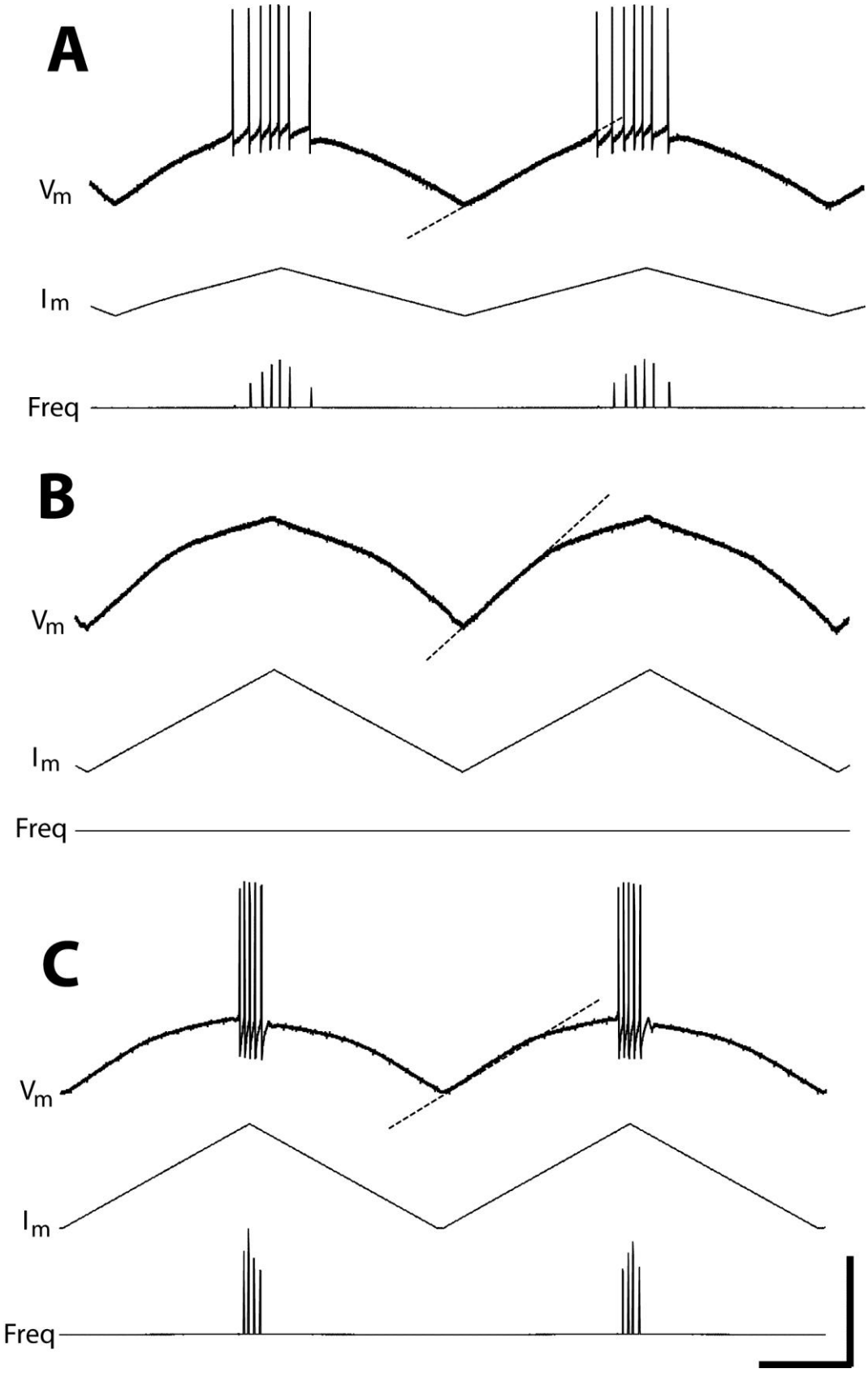
A
Vm
Im
Freq
B
Vm
Im
Freq
C
Vm
Im
Freq

Figure 8. Transient depolarization and delayed membrane repolarization at the beginning of a depolarizing current pulse were not appreciably altered by blockers for sodium and calcium voltage-gated channels, but were substantially reduced by blocking voltage-gated potassium channels. Membrane potential (V_m) of an injured I1 neuron in response to symmetrical hyperpolarizing and depolarizing 0.2s current pulses (I_m). Same I1 neuron was recorded for all traces, and drugs were sequentially added to the bath without removing the micropipette from the neuron. (A1) Change in membrane potential (V_m) in response to current pulses (I_m) and (A2) V-I plot with no drugs in the bath. Solid line = V_m for steady state at the end of the depolarizing current pulse. Dashed line = V_m for the peak of the transient depolarization, before the delayed repolarization. (B1, B2) Responses after adding 3 μM TTX, 400 μM $NiCl_2$, and 200 μM $CdCl_2$, and (C1, C2) after adding 10 mM TEA, and 5 mM 4-AP. Vertical/horizontal scale bars = 15 mV, 7.5 nA/0.05 s.

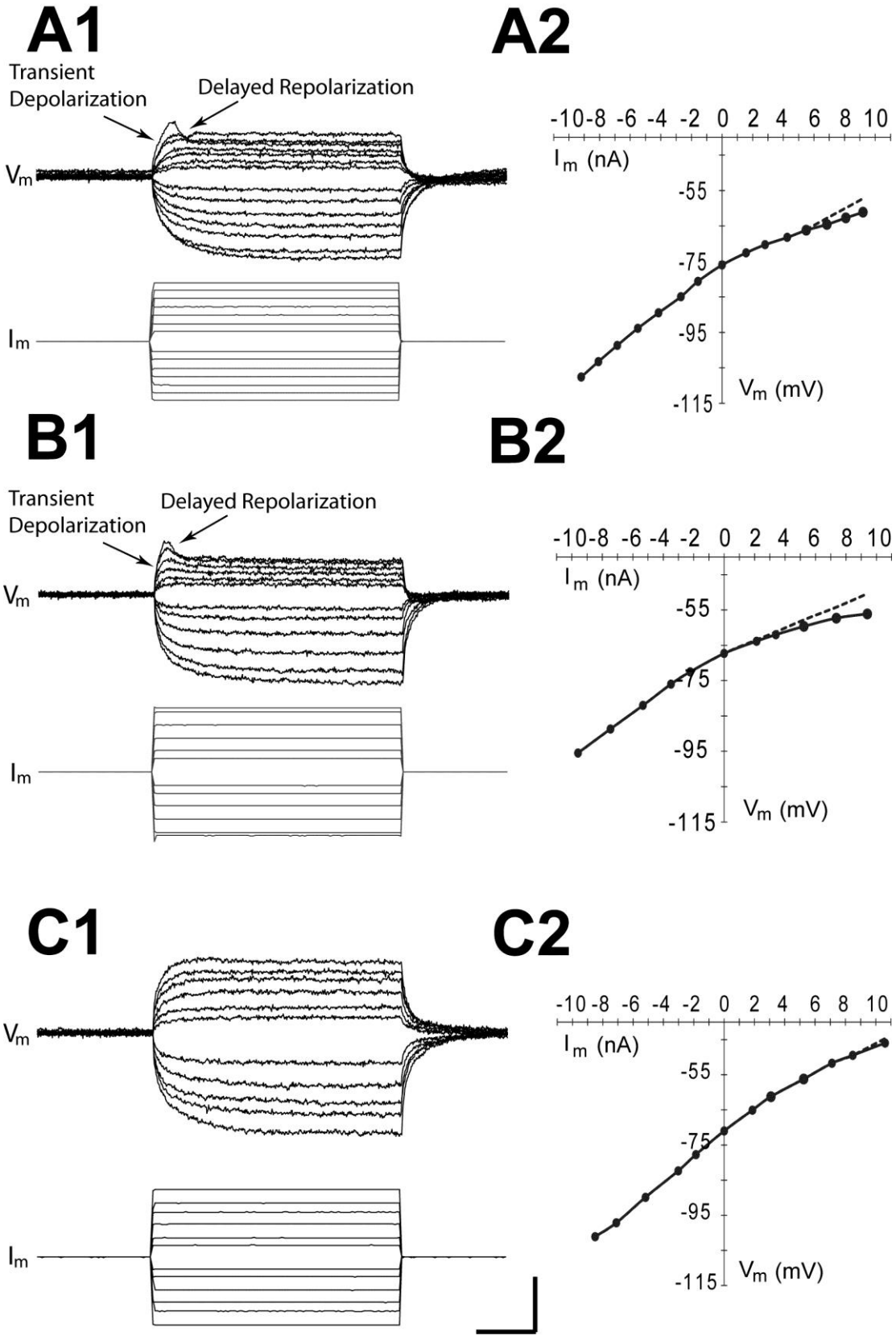
A1
Transient Depolarization
Delayed Repolarization
Vm
Im
A2
-10 -8 -6 -4 -2 0 2 4 6 8 10
Im (nA)
-55
-75
-95
-115
Vm (mV)
B1
Transient Depolarization
Delayed Repolarization
Vm
Im
B2
-10 -8 -6 -4 -2 0 2 4 6 8 10
Im (nA)
-55
-75
-95
-115
Vm (mV)
C1
Vm
Im
C2
-10 -8 -6 -4 -2 0 2 4 6 8 10
Im (nA)
-55
-75
-95
-115
Vm (mV)

Figure 9. Membrane potential (V_m) of injured RS neurons in response to 2.0 s depolarizing current pulse (I_m) in the presence of 0.5 mM KYN showing various sizes of transient depolarization and subsequent delayed repolarization (insets), and the corresponding firing patterns. (A1) Injured I3 neuron that displayed no delayed repolarization (inset) in response to a just sub-threshold depolarizing current pulse, and (A2) a smooth train of APs in response to a supra-threshold current pulse. (B1) Injured B1 neuron that displayed a small delayed repolarization (inset) in response to a just sub-threshold depolarizing current pulse, and (B2) short bursts of APs in response to a supra-threshold current pulse. Note resonance between bursts (arrowhead). (C1) Injured B4 neuron that displayed moderate delayed repolarization (inset) in response to a just sub-threshold depolarizing current pulse, and (C2) a single, short burst of APs in response to a supra-threshold current pulse. Note short resonance-like response following the burst (arrowhead). (D1) Injured B3 neuron that displayed a large delayed repolarization (inset) in response to a just sub-threshold depolarizing current pulse, and (D2) only one AP in response to a supra-threshold current pulse. The # in the inset for D1 indicates the approximate "time course" of the delayed repolarization (see Table 2), from the peak of the transient depolarization to the V_m following the initial, rapid membrane repolarization. Vertical/horizontal scale bars = 25 mV, 10 nA/0.5 s. Insets enlarged by 2.0x. The APs are clipped for A2, B2, C2, and D2 (horizontal dashed lines).

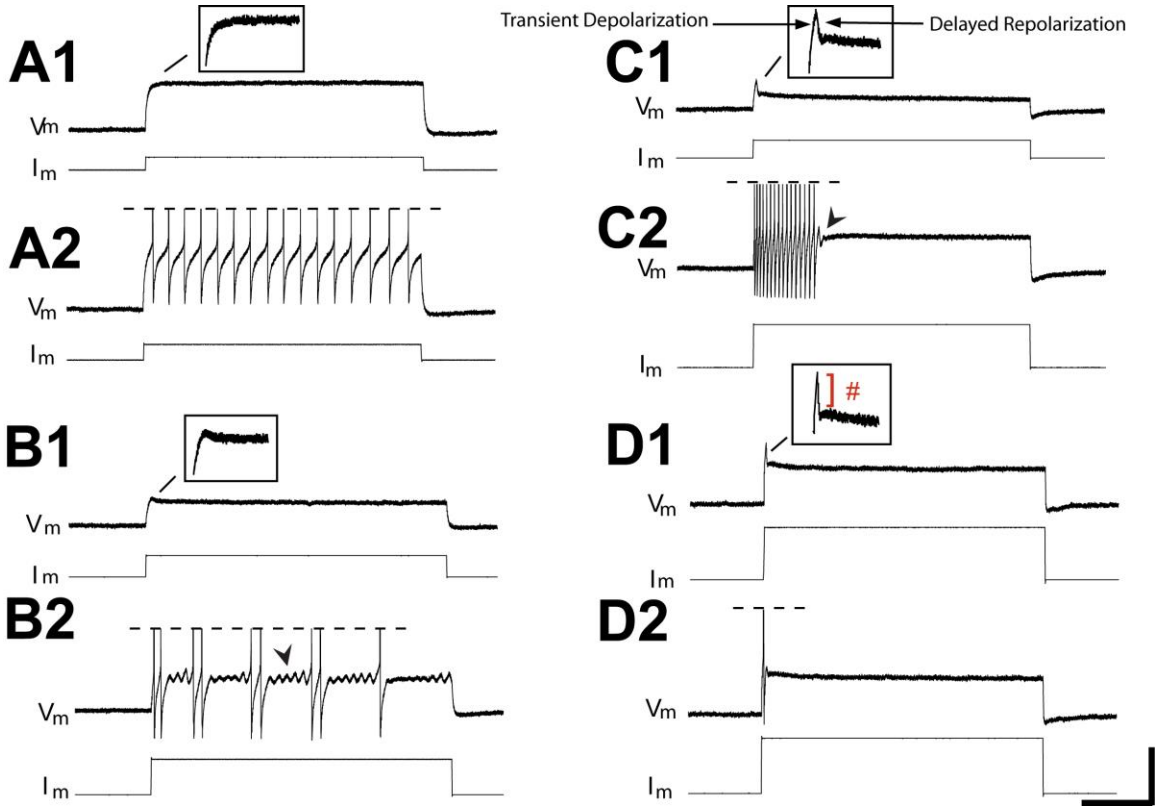
A1
Vm
Im
A2
Vm
Im
B1
Vm
Im
B2
Vm
Im
Transient Depolarization
Delayed Repolarization
C1
Vm
Im
C2
Vm
Im
#
D1
Vm
Im
D2
Vm
Im

Figure 10. Membrane current (I_m) in response to voltage pulses (V_m) in the presence of 0.5 mM KYN. (A) Voltage clamp recordings from an uninjured I1 neuron, which was held at V_{rest} (-71.75 mV), showing no activation of an outward current at sub-threshold voltages. (B) Voltage clamp recordings from an injured I1 neuron, which was held at V_{rest} (-69.62 mV), showing activation of an outward current at sub-threshold voltages. (C) I-V plots for the neurons in A and B showing activation of outward current at sub-threshold voltages for injured I1 neuron (closed circles) but not for uninjured I1 neuron (open circles). Vertical dashed lines = V_{th}. Vertical/horizontal scale bars = 6.67 nA, 20 mV/0.2 s.

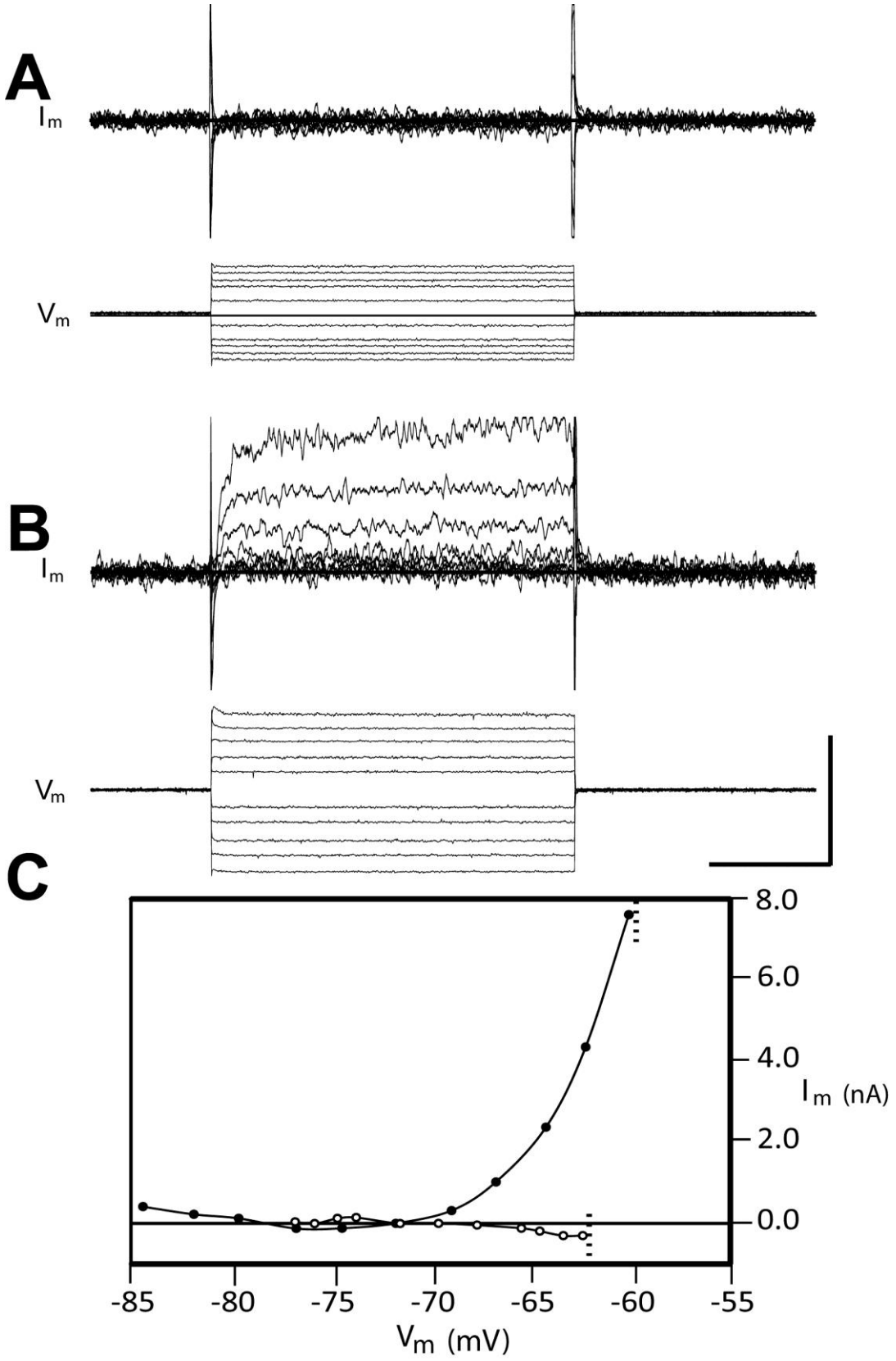
A
Im
Vm
B
Im
Vm
C
8.0
6.0
4.0
2.0
0.0
Im (nA)
-85
-80
-75
-70
-65
-60
-55
Vm (mV)

Figure 11. Voltage clamp recordings of membrane currents (I_m) for an uninjured and injured RS neurons in response to voltage pulses (V_m) in the presence of 3 μM TTX, 400 μM $NiCl_2$, and 200 μM $CdCl_2$. (A) Voltage clamp recordings from an uninjured I1 neuron, which was held at Vrest -69.29 mV), showing activation of a delayed outward current for depolarizing voltage pulses. (B) Voltage clamp recording of an injured B3 neuron, which was held at V_{rest} (-69.29 mV), showing activation of a delayed outward current for depolarizing voltage pulses. (C) I-V plots for the uninjured I1 neuron (open circles) and injured B3 neuron (closed circles) showed a more hyperpolarized effective activation voltage of the outward current for injured RS neurons as compared to uninjured RS neurons (see Fig. 12). These two neurons were selected because they had similar V_{rest} values. The red line indicates that scaling the currents for the I-V plot for uninjured I1 neuron by a factor of 12 resulted in a good match to the currents for the injured B3 neuron. Dashed lines indicate linear regression through last three points for each plot to estimate the effective activation voltages (V_K; arrows) for the delayed outward current (see Methods and Discussion). Vertical/horizontal scale bars = 10 nA, 20 mV/0.2 s.

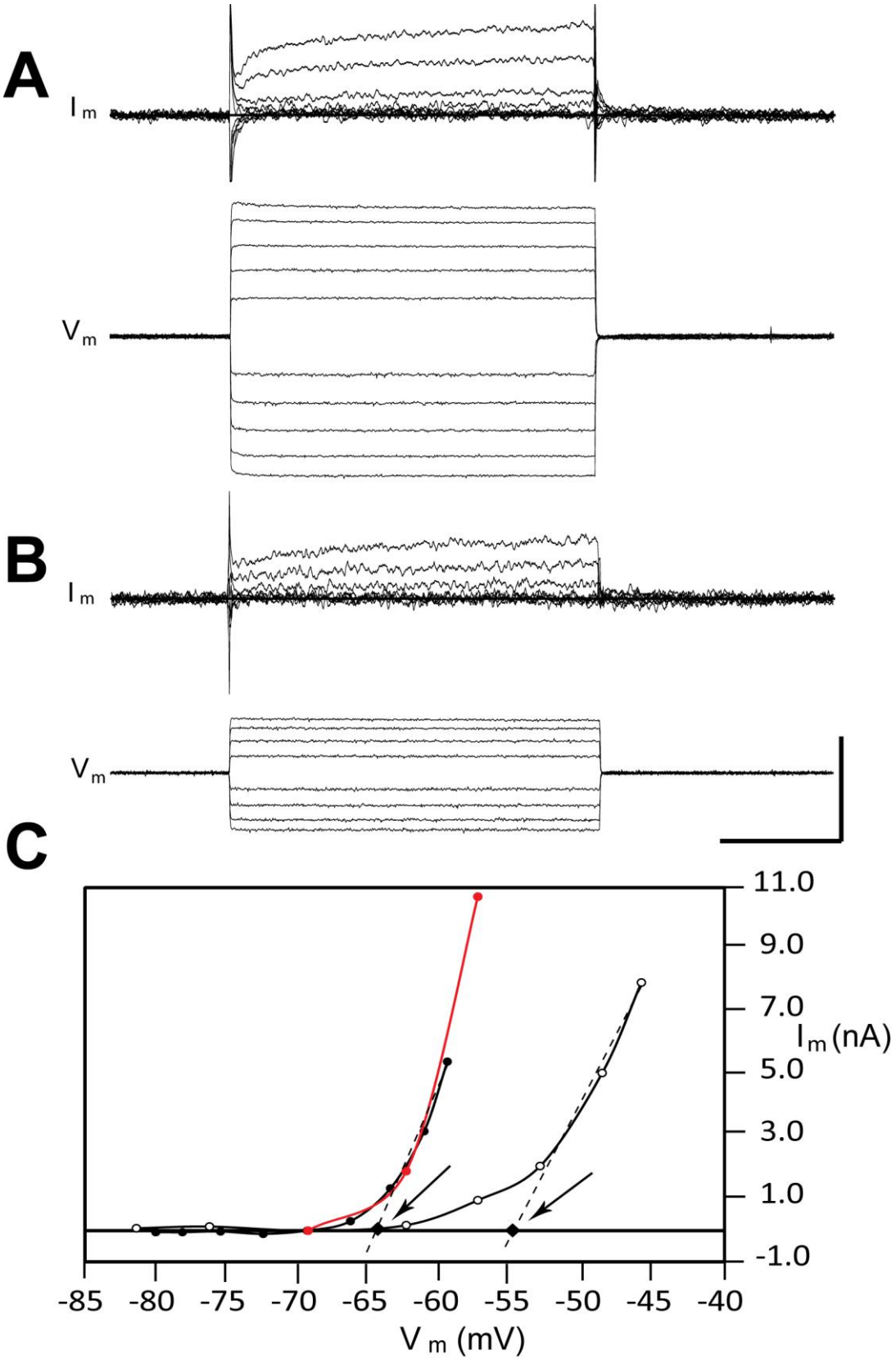
A
Im
Vm
B
Im
Vm
C
11.0
9.0
7.0
5.0
3.0
1.0
-1.0
Im (nA)
-85
-80
-75
-70
-65
-60
-55
-50
-45
-40
Vm (mV)

Figure 12. Histograms showing the differences in properties of uninjured (N = 23) and injured (N = 17) RS neurons recorded in the presence of 3 μM TTX, 400 μM $NiCl_2$, and 200 μM $CdCl_2$. (A) Resting membrane potential (V_{rest}) for uninjured and injured RS neurons was not significantly different. (B) Membrane potential (V_m) for the effective activation voltage (V_K) of the delayed outward current was at a significantly more hyperpolarized V_m for injured RS neurons as compared to uninjured RS neurons. (C) Amplitude of the depolarization ($V_{rest} \rightarrow V_K$) for activating the delayed outward current was significantly smaller for injured RS neurons as compared to that for uninjured RS neurons. (*** – $p < 0.001$, unpaired t-test with Welch correction).

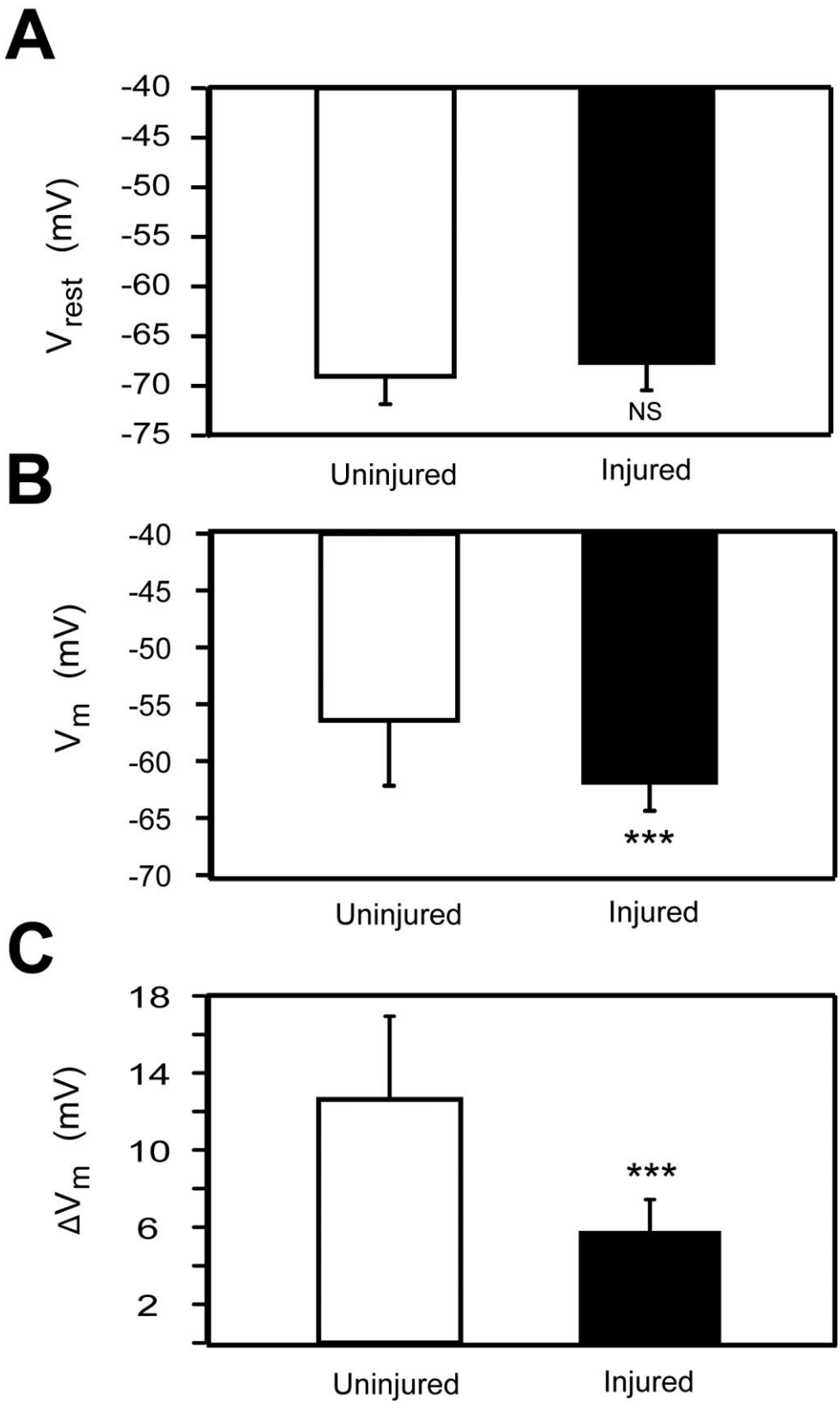
A
-40
-45
-50
-55
-60
-65
-70
-75
V_{rest} (mV)
NS
Uninjured
Injured
B
-40
-45
-50
-55
-60
-65
-70
V_m (mV)
***
Uninjured
Injured
C
18
14
10
6
2
ΔV_m (mV)
***
Uninjured
Injured

Figure 13. I-V plot for an injured B1 neuron in the presence of 3 μM TTX, 400 μM $NiCl_2$, and 200 μM $CdCl_2$ before (closed circles) and after (open circles) the application of 10 mM TEA and 5 mM 4-AP. Dashed line shows that scaling the current after the application of TEA and 4-AP (open circles) by a factor of 16 resulted in a plot that closely matched the I-V plot prior to application of K^+ channel blockers (closed circles).

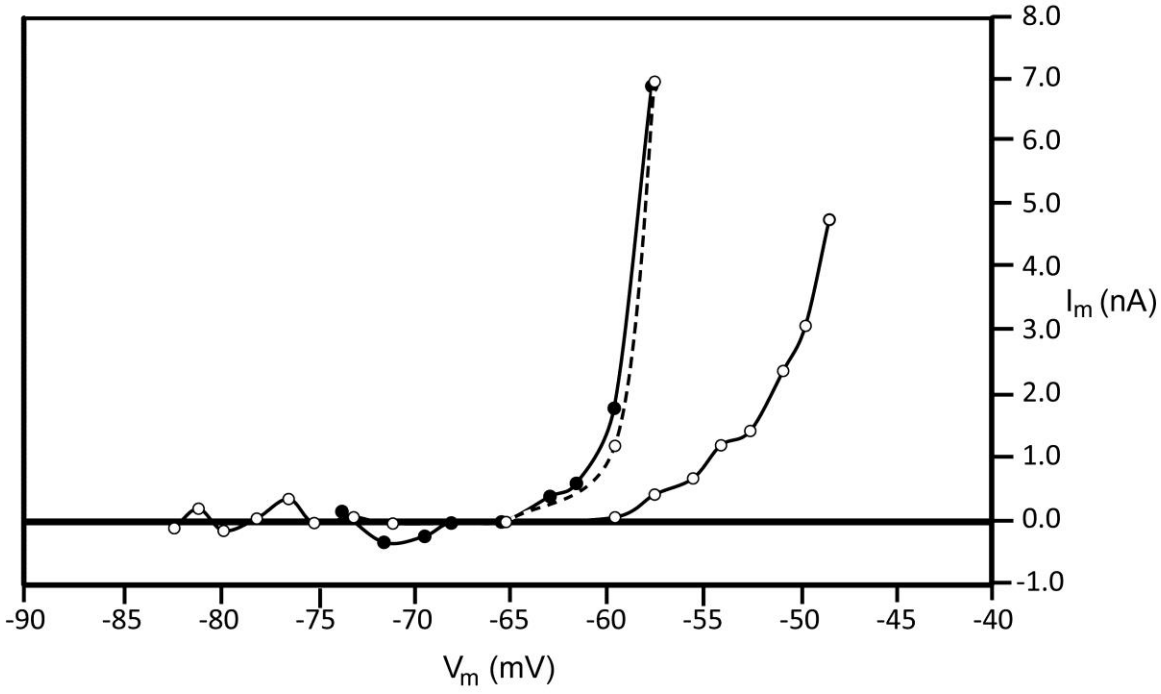
8.0
7.0
6.0
5.0
4.0
3.0
2.0
1.0
0.0
-1.0
I_m (nA)
-90
-85
-80
-75
-70
-65
-60
-55
-50
-45
-40
V_m (mV)

Figure 14. Time course of the effect of applying 3 μM TTX to the bath for an uninjured B1 neuron (see Methods). (A) Before application of TTX, uninjured B1 neuron fired a smooth train of APs in response to a 2.0 s depolarizing current pulse. (B) After application of TTX, and before a complete block of voltage-gated sodium channels (see Methods), uninjured B1 neuron displayed multiple bursts and membrane resonance (inset). (C) After the concentration of TTX had further increased around the brain and more voltage-gated sodium channels were blocked, the firing pattern changed from multiple bursts to a single burst, and the neuron displayed transient membrane potential oscillations (inset). Note: Partial block of voltage-gated sodium channels occurred ~60 minutes after adding TTX, and after ~70 minutes, TTX completely blocked APs. Vertical/horizontal scale bars = 60 mV, 12.5 nA, 25 Hz/0.5 s. Insets enlarged by 2.0x.

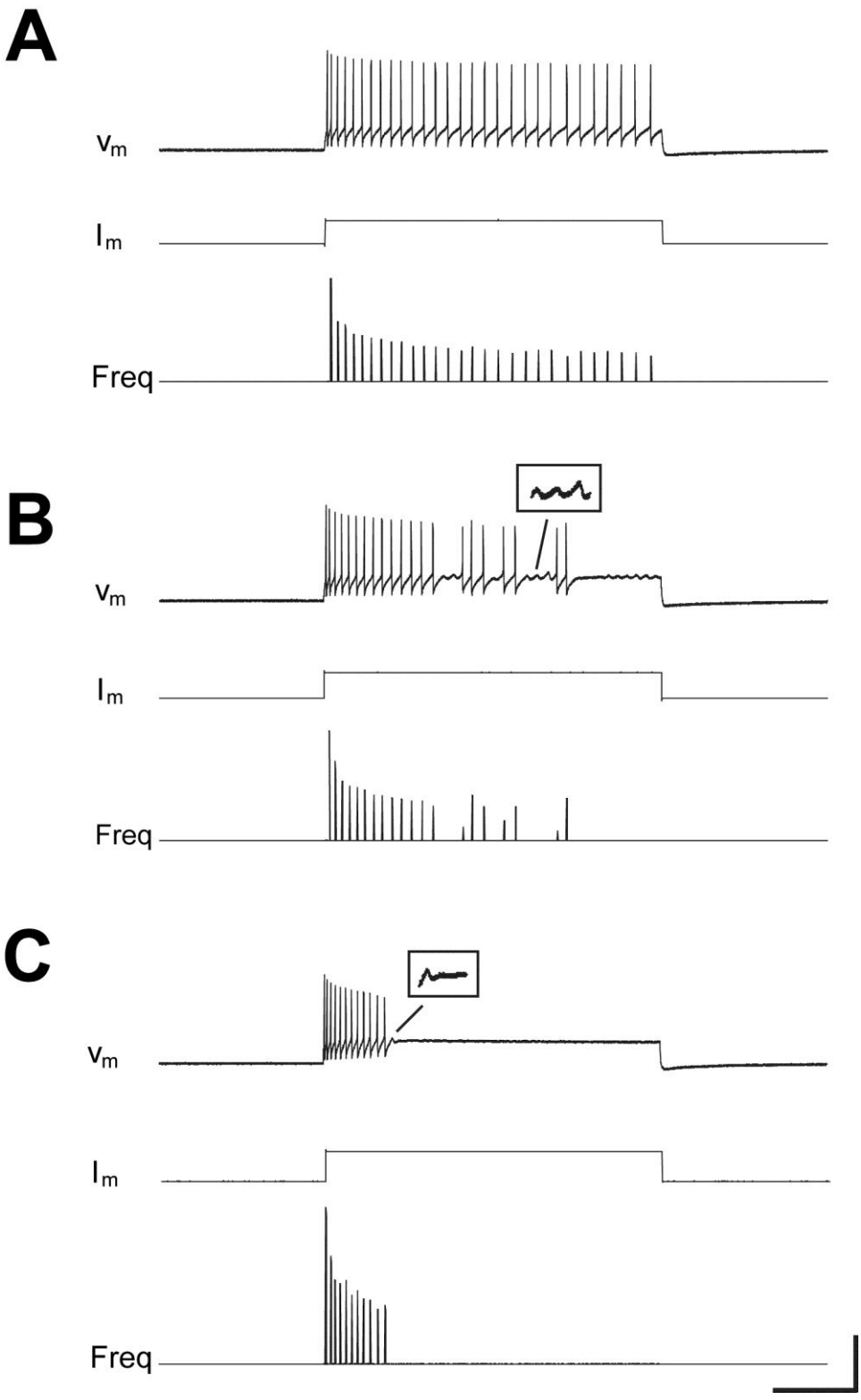
A
v_m
I_m
Freq
B
v_m
I_m
Freq
C
v_m
I_m
Freq

Figure 15. Effects of blocking SK channels with 1 μM UCL 1684 and partially blocking voltage-gated sodium channels with 150 pM TTX for an uninjured RS neuron. (A1) Uninjured B1 neuron fired a smooth train of APs before drug application and (A2) displayed short, repetitive bursting after application of the drugs. (B1) Uninjured B3 neuron fired a smooth train of APs before drug application and (B2) generated a single burst of APs after application of the drugs and a weak, short-duration membrane oscillation following the burst (see inset). (C) Uninjured I1 neuron that fired multiple bursts of APs in the presence of low dose TTX and also displayed membrane resonance (see inset). Vertical/horizontal scale bars = 120 mV, 10 nA, 50 Hz/1 s. Insets enlarged by 4.0x.

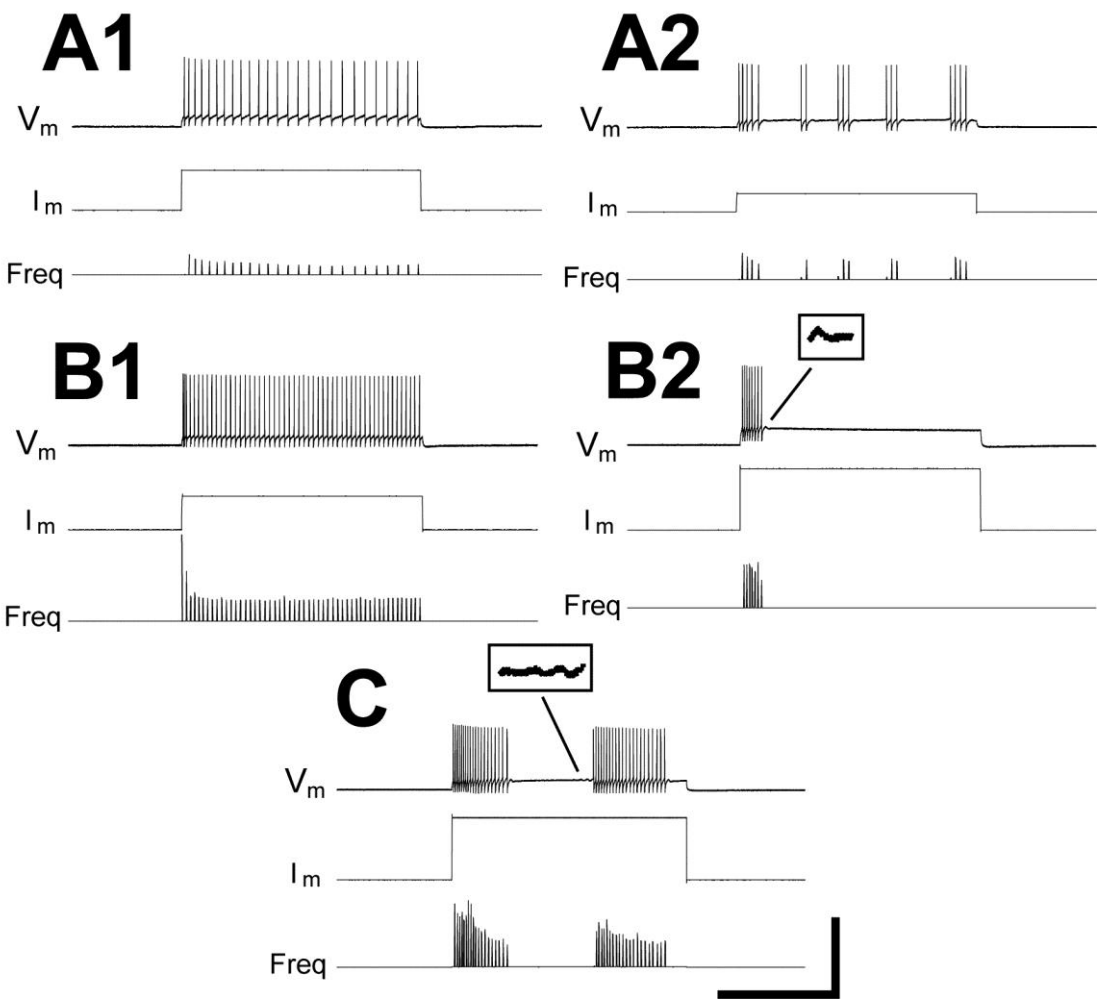
A1
Vm
Im
Freq
A2
Vm
Im
Freq
B1
Vm
Im
Freq
B2
Vm
Im
Freq
C
Vm
Im
Freq

Table 1
Biophysical Properties of Uninjured and Injured RS neurons

Action Potential Properties

	V_{rest} (mV)	V_{th} (mV)	V_{AP} (mV)	dV_m/dt_{rise} (mV/ms)	dV_m/dt_{fall} (mV/ms)	D_{AP} (ms)
Uninjured	-72.57 ± 4.33[a] (N = 128)[b]	-61.00 ± 4.47 (N = 113)	103.86 ± 7.22 (N = 128)	260.32 ± 34.25 (N = 127)	-138.95 ± 27.02 (N = 127)	0.97 ± 0.17 (N = 128)
Injured	-72.60 ± 4.89 (N = 84)	-57.65 ± 4.85*** (N = 77)	108.79 ± 7.60*** (N = 84)	268.81 ± 52.83 (N = 84)	-149.75 ± 24.09* (N = 84)	1.01 ± 0.14 (N = 84)

Afterpotential Properties

	V_{fAHP} (mV)	V_{ADP} (mV)	V_{sAHP} (mV)
Uninjured	-4.57 ± 2.92 (N = 108)	2.88 ± 1.98 (N = 91)	-1.49 ± 1.24 (N = 121)
Injured	-12.33 ± 4.31*** (N = 84)	0.07 ± 0.29*** (N = 76)	-0.08 ± 0.29*** (N = 81)

Passive Properties

	R_m (MΩ)	τ_m (ms)	C_m (pF)	R_{in} (MΩ)	τ_{in} (ms)	C_{in} (pF)
Uninjured	3.34 ± 2.57 (N = 118)	16.08 ± 8.03 (N = 118)	7.39 ± 8.13 (N = 118)	6.01 ± 3.85 (N = 118)	7.45 ± 3.59 (N = 118)	1.60 ± 1.05 (N = 118)
Injured	2.62 ± 1.48 (N = 81)	19.37 ± 11.88 (N = 81)	8.85 ± 6.88* (N = 80)	4.39 ± 1.98** (N = 81)	9.67 ± 4.79*** (N = 81)	2.36 ± 1.20*** (N = 81)

a – mean ± SD
b – number of neurons

Statistics: Comparisons between uninjured and injured RS neurons. * – $p \leq 0.05$, ** – $p \leq 0.01$, *** – $p \leq 0.001$. One-way ANOVA with Bonferroni multiple comparison post-test, or Kruskal-Wallis test with Dunn multiple comparison post-test.

Table 2
Properties of Delayed Repolarization for Injured RS Neurons Corresponding to Different Firing Patterns

Firing Pattern[a]	% of Total	Amplitude (mV)[b]	Delay of Onset (ms)[c]	Time Course (ms)[d]
Smooth Train	4.2	0.59 ± 0.84[e] (N = 3)[f]	34.52 ± 0.0 (N = 1)	28.92 ± 0.0 (N = 1)
Multiple Bursts	25.0	2.95 ± 2.11 (N = 18)	40.46 ± 10.48 (N = 18)	29.47 ± 10.54 (N = 15)
Single Burst	62.5	4.91 ± 2.08** (N = 45)	27.62 ± 8.88*** (N = 45)	22.67 ± 6.05** (N = 44)
Single AP	8.3	6.38 ± 2.12 (N = 6)	14.99 ± 7.60†† (N = 7)	12.73 ± 3.87†† (N = 6)

a – firing patterns for injured RS neurons (see Methods)
b – amplitude of delayed repolarization (peak of transient depolarization to steady-state membrane potential; see Figs. 5B1, 8A1)
c – delay from beginning of current pulse to the peak of the transient depolarization (onset of delayed membrane repolarization)
d – time from peak of transient depolarization to V_m following initial, rapid delayed repolarization (see insets in Fig. 9C1,D1)
e – mean ± SD
f – number of neurons

Statistics: Comparisons between neurons with multiple burst and single burst (*), and between neurons with single burst and single AP (†). *, † – $p \leq 0.05$, **, †† – $p \leq 0.01$, ***, ††† – $p \leq 0.001$. One-way ANOVA with Tukey multiple comparisons post-test.

Table 3
Biophysical Properties of Uninjured RS Neurons during a Partial Block of Voltage-Gated Sodium Channels[a]

Action Potential Properties

V_{rest} (mV)	V_{th} (mV)	V_{AP} (mV)	dV_m/dt_{rise} (mV/ms)	dV_m/dt_{fall} (mV/ms)	D_{AP} (ms)
-70.13 ± 3.34 [b] (N = 21) [c]	-60.53 ± 3.91 (N = 17)	98.28 ± 6.48**††† (N = 21)	244.81 ± 41.13 (N = 21)	-136.63 ± 26.34 (N = 21)	0.93 ± 0.14 (N = 21)

Afterpotential Properties

V_{fAHP} (mV)	V_{ADP} (mV)	V_{sAHP} (mV)
-4.62 ± 1.88††† (N = 18)	1.86 ± 1.51††† (N = 19)	-0.12 ± 0.35*** (N = 20)

Passive Properties

R_m (MΩ)	τ_m (ms)	C_m (pF)	R_{in} (MΩ)	τ_{in} (ms)	C_{in} (pF)
3.12 ± 2.39 (N = 12)	14.39 ± 10.21 (N = 12)	7.16 ± 6.66 (N = 12)	4.88 ± 3.13 (N = 12)	8.08 ± 3.22 (N = 12)	2.26 ± 1.29 (N = 12)

a – in addition to 150 pM TTX, 1 μM UCL was added to the bath to block SK channels
b – mean ± SD
c – number of neurons

Statistics: Comparisons to uninjured (*) and injured (†) RS neurons. *, † – $p \leq 0.05$, **, †† – $p \leq 0.01$, ***, ††† – $p \leq 0.001$. One-way ANOVA with Bonferroni multiple comparison post-test, or Kruskal-Wallis test with Dunn multiple comparison post-test.

DISCUSSION

Injury Phenotype for Lamprey RS Neurons

Previous studies had demonstrated that following SCI for the lamprey, injured RS neurons display a number of dramatic changes in their properties, described as the "injury phenotype", compared to uninjured neurons (McClellan, 2003,2009; McClellan et al., 2008): (a) altered firing patterns; (b) changes in afterpotential components; (c) reduction in excitability; and (d) down-regulation of SK channels and HVA calcium channels. These changes are thought to reduce calcium influx for injured RS neurons and provide a supportive intracellular environment for axonal regeneration (McClellan, 2013). The data from the present study confirmed and greatly extended the above findings regarding the underlying neuronal mechanisms for the "injury phenotype", as described below.

Changes in basic biophysical properties for injured RS neurons. In the present study, neurophysiological experiments indicated that relative to uninjured lamprey RS neurons, injured neurons display several dramatic changes in their biophysical properties: (a) decreased resistance (R_{in} and R_m), and increased capacitance (C_{in} and C_m) and time constant (τ_{in} and τ_m); (b) increased voltages (V_{th}) and current thresholds; (c) larger amplitudes for action potentials (V_{AP}); and (d) higher slope of the repolarizing phase of action potentials (dV_m/dt_{fall}). Several of these changes in properties are expected to reduce excitability of injured RS neurons relative to uninjured neurons.

Delayed repolarization and outward rectifying potassium channel. For the present study, it was found that for depolarized membrane potentials below and above V_{th}, injured lamprey RS neurons displayed a transient depolarization, which could elicit action potentials, following by a delayed repolarization, which counteracted

depolarization and could terminate or reduce firing (Fig. 5,9). The delayed repolarization resulted in non-linear V-I plots for depolarized membrane potentials below and above V_{th} (Fig. 5). Voltage clamp recordings suggest that the delayed repolarization was due to a delayed outward current that was activated for depolarized potentials below and above V_{th}. The delayed repolarization and delayed outward current were reduced by TEA and 4-AP, suggesting that both were very likely due to a delayed outward rectifying K^+ channel (Fig. 8,13), similar to or perhaps the same as the one that repolarizes the action potential. In contrast, although uninjured RS neurons also displayed delayed repolarization and delayed outward currents (Fig. 5,11), this was evident mostly for depolarized membrane potentials above V_{th}. Also, for injured neurons, the effective activation voltage for the delayed outward rectifying K^+ current was more hyperpolarized than that for uninjured neurons (Fig. 11) (see below). Taken together, the present results suggest that the delayed repolarization and outward rectifying K+ current for injured RS neurons will contribute to a reduction in excitability compared to that for uninjured neurons, and this is expected to reduce calcium influx.

In theory, the differences for the I-V plots for injured compared to uninjured RS neurons (Fig. 11) might be due to at least three mechanisms: (a) hyperpolarizing shift of the potassium equilibrium potential (E_K) for injured neurons; (b) hyperpolarizing shift in the "effective activation voltage" (V_K) for the delayed outward current for injured neurons; and/or (c) increase in the conductance (g_K) of the outward rectifying K^+ channel for injured neurons. First, V_{rest} was not significantly different for uninjured and injured RS neurons (Table 1), suggesting that a shift in E_K was unlikely. Second, a scaled version of the outward current for uninjured RS neurons closely matched the I-V plot of

outward current for injured neurons (see Fig. 11C and Results), suggesting that a shift in V_K was unlikely. Third, for injured RS neurons, there was an increase in the fAHP and dV_m/dt_{fall} (Table 1), both of which are dependent on delayed outward K^+ channels. Thus, it is likely that the larger delayed outward K^+ current for injured RS neurons compared to uninjured neurons mainly was due to an increase in g_K for the channel rather than a substantial change in kinetics. However, more complete I-V plots for injured and uninjured RS neurons, perhaps with the use of two-electrode voltage clamp (TEVC) or whole-cell patch clamp techniques, would be necessary to completely resolve this issue.

The delayed outward K^+ current activated fairly rapidly at membrane potentials near V_{th}, did not appear to inactivate appreciably by ~600-2000 ms at Vm of -60 mV, and was reduced but not blocked by TEA and 4-AP (Figs. 10,11,13), which are broad-spectrum K^+ channel blockers (Mathie et al., 1998; Magura et al., 2004; Roux 2005). These results suggest that the delayed outward current probably is associated with one or more of the delayed rectifier Kv channel subtypes but not Kv4.x, which underlie transient, fast inactivating A-current (Gutman et al., 2005; Rudy et al., 2009). The Kv1.x (Shaker-like) channel subtypes usually display inactivation and are mostly sensitive to 4-AP and high TEA (Gutman et al., 2005). The Kv7.1 channel subtypes typically are not blocked by 4-AP, require TEA levels of >30 mM for a substantial block, and are most effectively blocked by M-channel blockers (Gutman et al., 2005; Rudy et al., 2009). It is likely that the delayed outward K+ current in the present study is mediated by Kv2.x (Shab-like) and/or Kv3.1 (Shaw-like). One of the difficulties in determining the specific channel(s) underlying the delayed outward K^+ current based on kinetics is that expression of some of the K^+ channel subtypes in oocytes from different animals appears to result in different

kinetics (Covarrubias et al., 1991). In addition, the delayed outward K^+ current discovered in the present study might be due to a combination of the above K^+ channel subtypes. It would be interesting to apply TEA or 4-AP separately to determine if there are differential effects on the delayed outward K^+ current. It also would be useful to try applying other possibly more specific K^+ channel blockers that are available from various chemical companies (e.g. Tocris, Abcam, Alomone Labs), provided the specificity and potency of the blockers are conserved for lamprey neurons. Also, ongoing molecular studies of mRNA expression of the various Kv channel subtypes for uninjured and injured lamprey RS neurons might shed light on the subtypes that contribute to the delay outward rectifying K^+ current.

Interestingly, the amplitude, delay, and time course of the delayed repolarization were correlated with the specific firing pattern displayed by injured RS neurons. At one extreme, little or no delayed repolarization was correlated with smooth firing. At the other extreme, substantial delayed repolarization was correlated with firing of a single burst or a single action potential, which are firing patterns displayed by ~70% of injured RS neurons. Thus, the delayed repolarization appears to dictate to a significant degree the specific firing pattern associated with the "injury phenotype" for a given neuron.

Induction of the "injury phenotype" for uninjured lamprey RS neurons. Relative to uninjured neurons, for injured neurons the fAHP and dV_m/dt_{fall} were both significantly larger, suggesting a relatively large increase for g_K, while V_{AP} was significantly larger but dV_m/dt_{rise} was not, suggesting a more moderate increase for g_{Na} (Table 1). These data suggest that for injured RS neurons there was a concurrent but differentially larger increase in g_K relative to g_{Na} following SCI compared to the conductance levels for

uninjured neurons. It was hypothesized that partially blocking sodium channels for *uninjured RS neurons*, to differentially reduce g_{Na} relative to g_K, might induce the injury phenotype.

For *uninjured RS neurons*, partially blocking voltage-gated sodium channels with a low dose of TTX (150 pM), as well as blocking SK channels with UCL 1684, could induce firing patterns and membrane resonance, similar to those of the "injury phenotype" (Fig. 14,15). Blocking SK channels will abolish the sAHP, which is largely absent for injured neurons (Fig. 4C2), and reduce SFA so that firing frequency is increased (El Manira et al., 1994). Partially blocking Na^+ channels and reducing g_{Na} relative to g_K might compromise the ability of uninjured neurons to engage in sustained firing. It would be interesting to apply low doses of TEA and/or 4-AP to injured RS neurons to determine if restoring a more normal balance between g_K and g_{Na} would counteract the injury phenotype and restore smooth firing.

Some of the sodium channel subtypes have relatively high sensitivities for TTX (Alexander et al., 2011). For example, Nav1.1-1.4, Nav1.6, and Nav1.7 all have IC50 values less than ~15 nM, while the other Nav channel subtypes have values of 1-60 μM. In addition, all of these particular sodium channel subtypes have activation voltages of approximately -20 to -40 mV, at least for mammals (Catterall et al., 2005). Thus, in the present study, the low dose of TTX may have partially blocked some or all of these sodium channel subtypes and contributed to the induction of injury-like firing and resonance for *uninjured neurons*.

Other points. Almost all uninjured RS neurons fired a smooth train of APs in response to a depolarizing current pulse, while most injured neurons displayed altered

firing patterns (Fig. 4,9). Some uninjured RS neurons (~2%) did not fire smoothly, however these neurons did not exhibit the typical single, short burst or multiple short bursts observed for injured RS neurons (Fig. 4B1,B2). It is possible that even though these RS neurons were recorded from lampreys that did not receive a SCI, the neurons might have had an atypical ion channel profile causing them to behave slightly different than normal. In addition, some injured neurons (~4.2%) did fire smoothly, possibly because these few neurons did not fully responded to axotomy or their axons sealed very quickly with limited injury current.

For injured RS neurons, sometimes it was observed that application of higher-frequency sine or triangular current waveforms elicited firing, while for the same neurons, lower frequency waveforms did not elicit firing. The lower frequency membrane potential oscillations might have allowed the delayed repolarization, mediated by a delayed outward K^+ rectifier channel(s), to more fully develop for each cycle, counteracted depolarization, and prevented firing. In contrast, for higher frequency membrane potential oscillations, the delayed repolarization might not have fully developed for each cycle, thus allowing the neuron to fire. Also, a more rapid depolarizing during higher frequency membrane potential oscillations would more effectively activate sodium channels and prevent concurrent inactivation.

Possible Mechanisms for the Injury Phenotype for Injured Lamprey RS Neurons

Recently published studies suggest that spinal synaptic targets of lamprey RS neurons supply neurotrophic support, and that SCI temporarily abolishes this neurotrophic support and triggers the injury phenotype as well as activates an axon growth state (Benes et al., 2017). During neurodevelopment, before RS neurons make

synapses with spinal neurons and obtain neurotrophic support, these neurons might be in a growth state similar to that following injury. Thus, SCI potentially could trigger recapitulation of a built-in developmental axon growth program and stimulate axotomized neurons to regenerate their axons in search of spinal targets and neurotrophic support. Following axonal regeneration and reconnection with spinal targets, neurotrophic support presumably would be restored and suppress further axonal growth, thus leading to the incomplete axonal regeneration displayed by lampreys following SCI (reviewed in McClellan, 1994,1998,2013).

Results from the present suggest that following SCI there is a differential increase in g_K compared to g_{Na} for injured RS neurons that is expected to reduce electrical excitability. If these increases in conductance are due to up-regulation of mRNA for the two channels, it is possible that there is co-regulation of gene expression for these particular channels, similar to that demonstrated for neurons in the stomatogastric ganglion (Schulz et al., 2007).

Contribution of Injury Phenotype to Axonal Regeneration of Lamprey RS Neurons

First, for lamprey RS neurons in culture, focal application of high-K media or glutamate to growth cones or neuronal cell bodies induces calcium influx that inhibits neurite outgrowth or can cause neurite retraction (Ryan et al., 2007). Thus, elevation of intracellular calcium appears to be detrimental for axonal outgrowth (reviewed in McClellan, 2013). Second, following SCI, lamprey RS neurons display a number of dramatic changes in iophysical properties compared to those of uninjured neurons (present study and reviewed in McClellan, 2013): (a) reduced membrane resistance; (b) higher voltage and current thresholds; (c) increase in delayed outward K^+ current; (d)

reduction in average firing frequency for a given depolarizing input; (e) membrane potential resonance; (f) changes in the afterpotential components following action potentials; and (g) down-regulation of HVA calcium and SK channels. Most of the above changes in biophysical properties will reduce excitability, which coupled with a down-regulation of calcium channels, will decrease calcium influx and/or prevent large increases in intracellular calcium levels for injured RS neurons compared to the conditions in uninjured neurons. Thus, these changes in biophysical properties of injured lamprey RS neurons appear to be critical for providing supportive intracellular conditions for axonal regeneration.

For many neurons in culture, there is a range of in intracellular calcium that supports axonal outgrowth, referred to the "calcium set-point hypothesis" (reviewed in Kater et al., 1988; Kater and Mills, 1991; Henley and Poo, 2004). Thus, increases in internal calcium levels above this range are detrimental to axonal growth. Interestingly, contact of growth cones of mammalian neurons in culture with mature myelin triggers calcium influx and growth cone collapse (Bandtlow et al., 1993), which can be blocked by calcium channel blockers (Moorman and Hume, 1993). Following SCI, the central, ascending axons of rat dorsal root ganglion (DRG) neurons are able to regenerate if their peripheral axonal branch has received a pre-conditioning axotomy, which abolishes neuronal activity and down-regulates Cav1.2 channels (Enes et al., 2010).

Comparisons to Axotomy of Other Neurons for the Lamprey

Besides the characterization of the biophysical properties of injured lamprey RS neurons following SCI (current study and reviewed in McClellan, 2013), the only other axotomized lamprey neurons that have been studied electrophysiologically are spinal

dorsal cells (DCs) (Yin et al., 1981), which are centrally located primary sensory neurons that mainly have ascending axons (Rovainen 1979). Compared to uninjured DCs, injured neurons displayed the following changes in electrical properties: (a) increase in R_{in}; (b) increase in voltage and current thresholds; (c) decreased dV_m/dt_{rise}; (d) increased D_{AP}; and (e) increased V_{AP}. Thus, except for the changes for V_{th} and V_{AP}, axotomized lamprey DCs appear to respond quite differently to injury compared to axotomized RS neurons. Part of this difference might be due to the very different functions, different intrinsic responses to injury, and/or different intracellular conditions for these two types of neurons. However, for both of these neuron types, distant axotomy (>30 mm) has substantially less effect in altering the electrical properties than does close axotomy (Yin et al., 1981; Benes et al., 2017).

Changes in Ion Channels for Axotomized Neurons in Other Preparations

The effects of axotomy on the electrical properties of neurons, ion channel currents, and channel expression have been widely studied. In general, axotomized neurons often display an increase in excitability, particular for sensory neurons, but overall the effects can be variable and depend on a number of factors, including the particular type of neuron, recovery time, proximity of the injury to the soma, and the nature of the injury.

Potassium channels. Following axotomy of B-cells in bullfrog sympathetic ganglia, there was an increase in M-conductance (muscarinic-sensitive, voltage-dependent K+ channels), a decrease in the delayed rectifier K^+ current, decreased fast, voltage-sensitive calcium-activated K+ current (BK), and decreased voltage-insensitive calcium-activated K^+ currents (SK) (Jassar et al., 1994). For axotomized rat dorsal root

ganglion (DRG) neurons (i.e. sensory), the expression for several Kv1.x, Kv2.x, and Kv4.x channel subtypes are decreased (Kim et al., 2002; Park et al., 2003).

Sodium channels. Axotomy of rat dorsal root ganglion (DRG) neurons (i.e. sensory neurons) resulted in an increase in excitability due, in part, to an increase in overall Na^+ current, but there was a reduction of slow inactivating TTX-resistant (TTX-R) Na^+ currents and an enhancement of fast inactivating TTX-sensitive (TTX-S) Na^+ currents (Rizzo et al., 1995). Another research study also showed an increase in excitability of these injured neurons, but there was an increase in sodium currents for both TTX-S and TTX-R channels and a slowing of sodium channel inactivation (Abdulla and Smith, 2002).

Calcium channels. For many studies of injured neurons, there is a decrease in calcium currents, conductances, and/or channel expression levels. For example, axotomy of rat DRG neurons resulted in a reduction of N-type HVA calcium channel currents and a depolarizing shift in channel inactivation (Baccei and Kocsis, 2000). Following axotomy of medium-size DRG neurons in mice, there was a reduction in HVA or LVA calcium channel currents depending on sensory neuron type (Andre et al., 2003).

Axotomy effects on multiple ion channels. For many neurons, axotomy alters currents and conductances for multiple ion channels. For example, axotomy of bullfrog sympathetic neurons resulted in a reduction of calcium currents (mainly via N-type calcium channels), increased sodium channel conductance, and reduced currents via calcium-activated potassium channels (Jassar et al., 1993). For axotomized rat DRG neurons, there was a decrease in HVA calcium currents, decrease in delayed rectifier K+ channels currents, decrease in I_H, and no change in calcium-activated potassium channel

currents, which together are thought to increase excitability (Abdulla and Smith, 2001).

Summary and Conclusions

The present study investigated many of the biophysical properties of uninjured lamprey RS neurons and how the properties change for injured neurons following SCI. Collectively, these altered properties of injured RS neurons are referred to as the "injury phenotype", and consist of changes in both active and passive electrical properties, as well as changes in the repetitive firing properties. Although determining the changes that characterize the "injury phenotype" is important, elucidating the possible neuronal mechanisms that underlie these changes might provide insight into how injured lamprey RS neurons create an environment that is supportive for axonal regeneration and that leads to behavioral recovery following SCI.

In the present study, it was found that injured RS neurons displayed a delayed membrane repolarization that was activated at just below and above threshold. The same delayed membrane repolarization appeared to be present for uninjured RS neurons, but was mostly evident above threshold. Voltage clamp recordings revealed that the delayed repolarization was mediated by a delayed outward current that was effectively activated at more hyperpolarized membrane potentials for injured RS neurons as compared to uninjured RS neurons. By sequentially adding different ion channel blockers, it was determined that the delayed outward current very likely was mediated by voltage-gated potassium channels. An outward rectifying potassium channel that activates sub-threshold for injured RS neurons would contribute to a reduction in neuronal excitability, which together with a down-regulation of calcium channels, would be expected to decrease calcium influx and provide supportive conditions for axonal regeneration (see

Introduction and Discussion).

Furthermore, we hypothesized that in addition to down-regulating HVA and SK channels, injured neurons also undergo substantial modulation of voltage-gated sodium and potassium channels. In particular, following SCI, injured lamprey RS neurons appeared to express a differential increase in conductance for potassium channels, which hyperpolarize the membrane, relative to that for sodium channels, which depolarize the membrane. To test this hypothesis, a low dose of TTX was applied to *uninjured* RS neurons to partially block voltage-gated sodium channels, thereby shifting the balance toward a larger potassium channel conductance. This manipulation induced *uninjured* RS neurons to adopt aspects of the "injury phenotype" such as injury-like repetitive firing patterns and membrane resonance.

Following SCI, injured lamprey RS neurons possess the remarkable ability to regenerate their axons across the spinal injury site and restore locomotor function in a few weeks. Therefore, it is important to understand how the biophysical properties of lamprey RS neurons change following SCI and how these changes might contribute to axonal regeneration. This information may yield clues as to how ion channel expression is modified following neuronal injury, and how those modifications optimize the cellular conditions for successful regeneration. This and other knowledge might provide insights into developing therapies to enhance the regenerative ability of neurons so as to possibly restore locomotion following SCI in higher vertebrates, including possibly one day, humans.

REFERENCES

Abdulla FA, Smith PA (2001) Axotomy- and autotomy-induced changes in Ca^{2+} and K^{+} channel currents of rat dorsal root ganglion neurons. J Neurophysiol 85: 644–658.

Abdulla FA, Smith PA (2002) Changes in Na+ channel currents of rat dorsal root ganglion neurons following axotomy and axotomy-induced autotomy. J Neurophysiol 88: 2518-2529.

Al-Mohanna FA, Cave J, Bolsover SR (1992) A narrow window of intracellular calcium concentration is optimal for neurite outgrowth in rat sensory neurones. Dev Brain Res 70: 287-290.

Alexander SPH, Mathie A, Peters JA (2011) Guide to receptors and channels. Brit J Pharm 164: S158-S160.

Andre S, Puech-Mallie S, Desmadryl G, Valmier J, Scamps F (2003) Axotomy differentially regulates voltage-gated calcium currents in mice sensory neurons. NeuroReport 14: 147–150.

Baccei ML, Kocsis JD (2000) Voltage-gated calcium currents in axotomized adult rat cutaneous afferent neurons. J Neurophysiol 83: 2227–2238.

Bandtlow CE, Schmidt MF, Hassinger TD, Schwab ME, Kater SB (1993) Role of intracellular calcium in NI-35 evoked collapse of neuronal growth cones. Science 259: 80–83

Bayev K, Beresovskii V, Kebkalo T, Savoskina L (1988) Afferent and efferent connections of brainstem locomotor regions: study by means of horseradish peroxidase transport technique. Neuroscience 26: 871-891.

Beattie MS, Hermann GE, Rogers RC, Bresnahan JC (2002) Cell death in models of spinal cord injury. Prog Brain Res 137: 37-47.

Becker T, Wullimann MF, Becker CG, Bernhardt RR, Schachner M (1997) Axonal regrowth after spinal cord transection in adult zebrafish. J Comp Neurol 377: 577-595.

Benes JA, House KN, Burks FN, Conaway KP, Julien DP, Donley JP, Iayamu MA, McClellan AD (2017) Regulation of axonal regeneration following spinal cord injury in the lamprey. J Neurophysiol (in press)

Benthall KN, Hough RA, McClellan AD (2017) Descending propriospinal neurons mediate restoration of locomotor function following spinal cord injury. J Neurophysiol 117: 215-229.

Bicker PE, Buck LT (2007) Hypoxia tolerance in reptiles, amphibians, and fishes: Life with variable oxygen availability. Annu Rev Physiol 69: 145-170.

Buchanan JT (2011) Spinal locomotor inputs to individually identified reticulospinal neurons in the lamprey. J Neurophysiol 106: 2346-2357.

Buchanan JT, Brodin L, Dale N, Grillner S (1987) Reticulospinal neurones activate excitatory amino acid receptors. Brain Res 408: 321-325.

Buchanan JT, Cohen AH (1982) Activities of identified interneurons, motoneurons, and muscle fibers during fictive swimming in the lamprey and effects of reticulospinal and dorsal cell stimulation. J Neurophysiol 47: 948-960.

Catterall WA, Goldin AL, Waxman SG (2005) Nomenclature and structure-function relationships of voltage-gated sodium channels. Pharm Rev 57: 397-409.

Cheng J, Magnuson DS (2011) Initiation of segmental locomotor-like activities by stimulation of ventrolateral funiculus in the neonatal rat. Exp Brain Res 214: 151-161.

Cohan CS, Kater SB (1986) Suppression of neurite elongation and growth cone mentality by electrical activity. Science 232: 1638-1641.

Covarrubias M, Wei A, Salkoff L (1991) Shaker, Shal, Shab, and Shaw express independent K+ current systems. Neuron 7: 763-773.

Davis BM, Ayers JL, Koran L, Carlson J, Anderson MC, Simpson SB (1990) Time course of salamander spinal cord regeneration and recovery of swimming: HRP retrograde pathway tracing and kinematic analysis. Exp Neurol 108: 198-213.

Davis GR, McClellan AD (1994a) Extent and time course of restoration of descending brainstem projections in spinal cord-transected lamprey. J Comp Neurol 344: 65-82.

Davis GR, McClellan AD (1994b) Long distance axonal regeneration of identified lamprey reticulospinal neurons. Exp Neurol 127: 94-105.

Davis GR, Troxel M, Kohler V, Grossmann E, McClellan A (1993) Time course of locomotor recovery and functional regeneration in spinal-transected lamprey: kinematics and electromyography. Exp Brain Res 97: 83-95.

Deliagina T, Zelenin P, Fagerstedt P, Grillner S, Orlovsky G (2000) Activity of reticulospinal neurons during locomotion in the freely behaving lamprey. J Neurophysiol 83: 853-863.

Dubuc R, Brocard F, Antri M, Fénelon K, Gariépy J.-F, Smetana R, Pearlstein É (2008) Initiation of locomotion in lampreys. Brain Res Rev 57: 172-182.

Eidelberg E, Story J, Walden J, Meyer B (1981) Anatomical correlates of return of locomotor function after partial spinal cord lesions in cats. Exp Brain Res 42: 81-88.

El Manira A, Pombal M, Grillner S (1997) Diencephalic projection to reticulospinal neurons involved in the initiation of locomotion in adult lampreys Lampetra fluviatilis. J Comp Neurol 389: 603-616.

El Manira A, Tégner J, Grillner S (1994) Calcium-dependent potassium channels play a critical role for burst termination in the locomotor network in lamprey. J Neurophysiol 72: 1852-1861.

Enes J, Langwieser N, Ruschel J, Carballosa-Gonzalez MM, Klug A, Traut MH et al (2010) Electrical activity suppresses axon growth through Cav1.2 channels in adult primary sensory neurons. Curr Biol 20: 1154–1164

Friesen W, Stent G (1978) Neural circuits for generating rhythmic movements. Ann Rev Biophys and Bioeng 7: 37-61.

Garcia-Rill E, Skinner R, Fitzgerald J (1983) Activity in the mesencephalic locomotor region during locomotion. Exp Neurol 82: 609-622.

Golowasch J, Thomas G, Taylor AL, Patel A, Pineda A, Khalil C, Nadim F (2009) Membrane capacitance measurements revisited: dependence of capacitance value on measurement method in nonisopotential neurons. J Neurophysiol 102: 2161-2175.

Grillner S, McClellan A, Perret C (1981) Entrainment of the spinal pattern generators for swimming by mechano-sensitive elements in the lamprey spinal cord in vitro. Brain Res 217: 380-386.

Grillner S, Wallen P (1985) Central pattern generators for locomotion, with special reference to vertebrates. Ann Rev Neurosci 8: 233-261.

Gutman GA, Chandy KG, Grissmer S, Lazdunski M, McKinnon D, Pardo LA, Robertson GA, Rudy B, Sanguinetti MC, Stuhmer W, Wang X (2005) Nomenclature and molecular relationships of voltage-gated potassium channels. Pharm Rev 57: 473-508.

Hagevik A, McClellan AD (1994) Coupling of spinal locomotor networks in larval lamprey revealed by receptor blockers for inhibitory amino acids: Neurophysiology and computer modeling. J Neurophysiol 72: 1810-1829.

Hasan SJ, Keirstead HS, Muir GD, Steeves JD (1993) Axonal regeneration contributes to repair of injured brainstem-spinal neurons in embryonic chick. J Neurosci 13: 492-507.

Henley J, Poo M-m (2004) Guiding neuronal growth cones using Ca 2+ signals. Trends Cell Bio 14: 320-330.

Holder N, Clarke J (1988) Is there a correlation between continuous neurogenesis and directed axon regeneration in the vertebrate nervous system? Trends Neurosci 11: 94-99.

Huang C-Y, Lien C-C, Cheng C-F, Yen T-Y, Chen C-J, Tsaur M-L (2017) K+ channel Kv3. 4 is essential for axon growth by limiting the influx of Ca^{2+} into growth cones. J Neurosci 37: 4433-4449.

Hunt D, Coffin R, Anderson P (2002) The Nogo receptor, its ligands and axonal regeneration in the spinal cord; a review. J Neurocytol 31: 93-120.

Jackson AW, Pino FA, Wiebe ED, McClellan AD (2007) Movements and muscle activity initiated by brain locomotor areas in semi-intact preparations from larval lamprey. J Neurophysiol 97: 3229-3241.

Jassar BS, Pennefather PS, Smith PA (1993) Changes in sodium and calcium channel activity following axotomy of B-cells in bullfrog sympathetic ganglion. J Physiol (Lond) 472: 203–231.

Jordan LM. (1986) Initiation of locomotion from the mammalian brainstem. In: Neurobiology of Vertebrate Locomotion (Eds Grillner S, Stein PG, Stuart DG, Forssberg H, Herman RM), Wenner-Gren Symposium Series Vol 45, MacMillan Press, London, pp. 21–37.

Kasicki S, Grillner S (1986) Müller cells and other reticulospinal neurones are phasically active during fictive locomotion in the isolated nervous system of the lamprey. Neurosci Lett 69: 239-243.

Kasicki S, Grillner S, Ohta Y, Brodin L (1989) Phasic modulation of reticulospinal neurones during fictive locomotion and other types of spinal motor activity in lamprey. Brain Res 484: 203-216.

Kater SB, Mattson MP, Cohan C, Connor J (1988) Calcium regulation of the neuronal growth cone. Trends Neurosci 11: 315-321.

Kater S, Mills L (1991) Regulation of growth cone behavior by calcium. J Neurosci 11: 891-899.

Kim DS, Choi JO, Rim HD, Cho HJ (2002) Downregulation of voltage-gated potassium channel α gene expression in dorsal root ganglia following chronic constriction injury of the rat sciatic nerve. Mol Brain Res 105: 146-152.

Lurie DI, Selzer ME (1991) Preferential regeneration of spinal axons through the scar in hemisected lamprey spinal cord. J Comp Neurol 313: 669-679.

Mackler S, Selzer M (1987) Specificity of synaptic regeneration in the spinal cord of the larval sea lamprey. J Physiol 388: 183-198.

Magura I, Kucher V, Boiko NY (2004) Voltage-operated potassium channels and mechanisms controlling their activity. Neurophysiol 36: 285-292.

Mathie A, Wooltorton JR, Watkins CS (1998) Voltage-activated potassium channels in mammalian neurons and their block by novel pharmacological agents. Gen Pharmac 30: 13-24.

Mattson MP, Kater SB (1987) Calcium regulation of neurite elongation and growth cone motility. J Neurosci 7: 4034-4043.

McClellan AD (1986) Command systems for initiating locomotor responses in fish and amphibians - Parallels to initiation of locomotion in mammals. In: Neurobiology of Vertebrate Locomotion, (Eds Grillner S, Stein P, Stuart D, Forssberg H, Herman R), Wenner-Gren Symposium Series Vol 45, MacMillan Press, London, pp. 3-20.

McClellan AD (1994) Functional regeneration and restoration of locomotor activity following spinal cord transection in the lamprey. Prog Brain Res 103: 203-217.

McClellan AD (1998) Spinal cord injury: Lessons from locomotor recovery and axonal regeneration in lower vertebrates. The Neuroscientist 4: 250-263.

McClellan AD (2003) Axotomy alters spike frequency adaptation of reticulospinal neurons in larval lamprey. Soc Neurosci Abst 29: 42.21.

McClellan AD (2009) Axotomized reticulospinal neurons in larval lamprey display changes in channel expression and firing activity. Soc Neurosci Abst 34: 766.15.

McClellan AD (2013) Spinal cord injury – The lamprey model. In: Animal Models of Spinal Cord Repair, (Ed. H Aldskogius), Neuromethods vol. 76, chap. 4, Humana Press, New York, pp. 63-108.

McClellan AD, Kovalenko MO, Benes JA, Schulz DJ (2008) Spinal cord injury induces changes in electrophysiological properties and ion channel expression of reticulospinal neurons in larval lamprey. J Neurosci 28: 650-659.

Moorman S, Hume RI (1993) Omega-conotoxin prevents myelin-evoked growth cone collapse in neonatal rat locus coeruleus neurons in vitro. J Neurosci 13: 4727-4736.

Mori S, Matsui T, Kuze B, Asanome M, Nakajima K, Matsuyama K (1998) Cerebellar-induced Locomotion: Reticulospinal control of spinal rhythm generating mechanism in cats. Ann NY Acad Sci 860: 94-105.

Mori S Shik M, Yagodnitsyn A (1977) Role of pontine tegmentum for locomotor control in mesencephalic cat. J Neurophysiol 40: 284-295.

Orlovskii G (1969) Spontaneous and induced locomotion of the thalamic cat. Biophysics 14: 1154-1162.

Orlovsky GN (1970) Connections between reticulospinal neurons and locomotor regions of the brain stem. Biofizika 15: 58-64.

Orlovsky GN, Deliagina TG, Grillner S (1999) Neuronal Control of Locomotion. Oxford, New York.

Paggett K, Jackson A, McClellan A (2004) Organization of higher-order brain areas that initiate locomotor activity in larval lamprey. Neuroscience 125: 25-33.

Park SY, Choi JY, Kim RU, Lee YS, Cho HJ, Kim DS (2003) Downregulation of voltage-gated potassium channel alpha gene expression by axotomy and neurotrophins in rat dorsal root ganglia. Mol Cells 16: 256-259.

Parker D, Grillner S (1996) Tachykinin-mediated modulation of sensory neurons, interneurons, and synaptic transmission in the lamprey spinal cord. J Neurophysiol 76: 4031-4039.

Rizzo MA, Kocsis JD, Waxman SG (1995) Selective loss of slow and enhancement of fast Na+ currents in cutaneous afferent dorsal root ganglion neurones following axotomy. Neurobiol Disease 2: 87-96.

Rouse DT, McClellan AD (1997) Descending propriospinal neurons in normal and spinal cord-transected lamprey. Exp Neurol 146: 113-124.

Rouse DT, Quan X, McClellan AD (1998) Biophysical properties of reticulospinal neurons in larval lamprey. Brain Res 779: 301-308.

Roux B (2005) Ion conduction and selectivity in K+ channels. Annu Rev Biophy Biomol Struct 34: 153-171.

Rovainen CM (1978) Müller cells, Mauthner cells, and other reticulospinal neurons in the lamprey. In: Neurobiology of the Mauthner Cell. (Eds D Faber, H Korn), Raven Press, New York, pp. 245-269.

Rovainen CM (1979) Neurobiology of lampreys. Physiol Rev 59: 1007-1076.

Rudy B, Maffie J, Amarillo Y, Clark B, Goldberg E, Jeong H, Zagha E (2009) Voltage gated potassium channels: Structure and function of Kv1 to Kv9 subfamilies. Encyclop Neurosci 10: 397-425.

Ryan SK, Shotts LR, Hong SK, Nehra D, Groat CR, Armstrong JR, McClellan AD (2007) Glutamate regulates neurite outgrowth of cultured descending brain neurons from larval lamprey. Dev Neurobiol 67: 173-188.

Schulz DJ, Goaillard J-M, Marder EE (2007) Quantitative expression profiling of identified neurons reveals cell-specific constraints on highly variable levels of gene expression. PNAS 104: 13187-13191.

Schwab ME (2004) Nogo and axon regeneration. Curr Op Neurobiol 14: 118-124.

Schwab ME, Bartholdi D (1996) Degeneration and regeneration of axons in the lesioned spinal cord. Physiol Rev 76: 319-370.

Shaw AC, Jackson AW, Holmes T, Thurman S, Davis G, McClellan AD (2010) Descending brain neurons in larval lamprey: Spinal projection patterns and initiation of locomotion. Exp Neurol 224: 527-541.

Shefchyk S, Jell R, Jordan L (1984) Reversible cooling of the brainstem reveals areas required for mesencephalic locomotor region evoked treadmill locomotion. Exp Brain Res 56: 257-262.

Shik M, Orlovskii G, Severin F (1968) Locomotion of mesencephalic cat elicited by stimulation of pyramids. Biophysics 13: 143-152.

Silver J, Horn K, Busch S, Yonkof A (2009) Axonal regeneration: Role of the extracellular matrix and the glial scar. Encyclop Neurosci 1173-1180.

Silver J, Miller JH (2004) Regeneration beyond the glial scar. Nat Rev Neurosci 5: 146-156.

Sirota MG, Di Prisco GV, Dubuc R (2000) Stimulation of the mesencephalic locomotor region elicits controlled swimming in semi-intact lampreys. Eur J Neurosci 12: 4081-4092.

Smith JJ, Kuraku S, Holt C, Sauka-Spengler T, Jiang N, Campbell MS, Bloom OE (2013) Sequencing of the sea lamprey (Petromyzon marinus) genome provides insights into vertebrate evolution. Nature Gen 45: 415-421.

Steeves JD, Jordan LM (1984) Autoradiographic demonstration of the projections from the mesencephalic locomotor region. Brain Res 307: 263-276.

Steeves JD, Keirstead HS, Ethell DW, Hasan SJ, Muir GD, Pataky DM, Zwimpfer TJ (1994) Permissive and restrictive periods for brainstem-spinal regeneration in the chick. Prog Brain Res 103: 243-262.

Steeves JD, Sholomenko GN, Webster DM (1987) Stimulation of the pontomedullary reticular formation initiates locomotion in decerebrate birds. Brain Res 401: 205-212.

Taylor J, Jack J, Easter S (1989) Is the capacity for optic nerve regeneration related to continued retinal ganglion cell production in the frog? Eur J Neurosci 1: 626-638.

Viala D (2006) Evolution and behavioral adaptation of locomotor pattern generators in vertebrates. Comptes Rendus Palevol 5: 667-674.

Walberg F, Pompeiano O, Brodal A, Jansen J (1962) The fastigiovestibular projection in the cat. An experimental study with silver impregnation methods. J Comp Neurol 118: 49-75.

Waller WH (1940) Progression movements elicited by subthalamic stimulation. J Neurophysiol 3: 300-307.

Whalley K, O'Neill P, Ferretti P (2006) Changes in response to spinal cord injury with development: vascularization, hemorrhage and apoptosis. Neuroscience 137: 821-832.

Wilkie MP (2011) Lampreys: Environmental physiology. Encylop Fish Physiology: From Genome to Environment, Vol 3, 1788-1799.

Wilson D, Waldron I (1968) Models for the generation of the motor output pattern in flying locusts. Proc IEEE 56: 1058-1064.

Yin HS, Wellerstein KK, Selzer ME (1981) Effects of axotomy on lamprey spinal neurons. Exp Neurol 73: 750-761.

Zelenin PV (2005) Activity of individual reticulospinal neurons during different forms of locomotion in the lamprey. Eur J Neurosci 22: 2271-2282.